Review

Strategies for area-selective deposition of metal nanoparticles on carbon nanotubes and their applications: a review

Fernanda Olivares[1,2], Francisco Peón[1,2], Ricardo Henríquez[3], and Rodrigo Segura del Río[1,*]

[1] Instituto de Química y Bioquímica, Facultad de Ciencias, Universidad de Valparaíso, Av. Gran Bretaña 1111, Valparaíso, Chile
[2] Doctorado Conjunto en Ciencias Mención Química, Universidad de Valparaíso - Universidad Técnica Federico Santa María, Valparaíso, Chile
[3] Departamento de Física, Universidad Técnica Federico Santa María, Avenida España, 1680 Valparaíso, Chile

ABSTRACT

Carbon nanotubes (CNTs) have a common use as a nanostructured substrate to support and stabilize metal nanoparticles (MNPs), generating hybrid materials whose properties can be a combination of individual materials' properties, generate synergistic effects, or even manifest new properties. Recently, it was reported that the physical and chemical properties of these hybrid nanomaterials vary depending on where the MNPs are deposited in the CNTs. This review will cover area-selective deposition types of MNP in the internal cavity of CNTs (I), on the external walls of CNTs (II), and at the ends of CNTs (III). Various methods have been developed for coupling these two nanomaterials in the three mentioned configurations, and this contribution presents a compilation of the most effective and their main characteristics. In this review, the characterization techniques that allow corroborating each method's selectivity are also mentioned, highlighting the most precise techniques. Finally, the areas in which these hybrid nanomaterials are being used are mentioned, as well as some applications in which the selective coupling of these could be important.

GRAPHICAL ABSTRACT
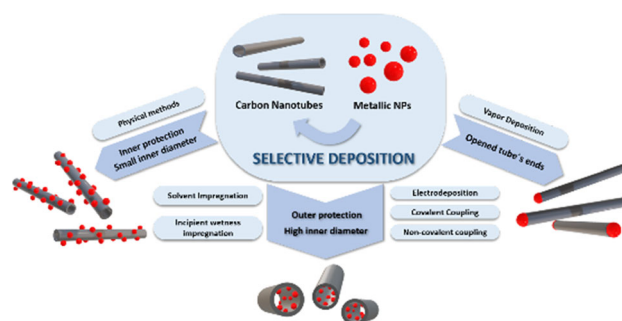
Abbreviations

|	
AAO	Anodized aluminum oxide
CA	Cinnamic alcohol
CALD	Cinnamaldehyde
CNT	Carbon nanotube
CVD	Chemical vapor deposition
EELS	Electron Energy-Loss Spectroscopy
EFTEM	Energy-filtered transmission electron microscopy
HCALD	Hydrocinnamaldehyde
MNP	Metal nanoparticle
MRI	Magnetic resonance imaging
MWCNT	Multi-wall carbon nanotubes
NCNTs	Nitrogen-doped CNTs
NP	Nanoparticle
OER	Oxygen evolution reaction
PP	Phenyl propanol
PVD	Physical vapor deposition
SMAD	Solvated metal atom dispersion
STEM-HAADF	Scanning Transmission Electron Microscopy-High Angle Annular Dark Field
SWCNT	Single-wall carbon nanotubes
TOF	Turnover frequency

Introduction

Carbon nanotubes (CNTs) are allotropic forms of carbon that present very interesting mechanical, electrical, and thermal properties [1–8]. Monthioux and Kuznetsov [9] stated that the existence of these nanomaterials had been demonstrated since the early 1970s when Wiles and Abrahamson [10] mentioned carbon fibers with diameters between 4 and 100 nm for the first time. Previously, in the same decade, Endo et al. proved the growth of carbon tubular structures of a few nanometers in diameter due to the catalytic decomposition of benzene in iron particles [11]. However, Iijima in 1991 mainly coined the term 'carbon nanotubes' in a study that sparked an explosion in CNT properties and applications research [12–14].

On the other hand, studying metal nanoparticles (MNPs) became prevalent because of their remarkable optical, electronic, and magnetic properties [15–21]. Among the phenomena that differentiate nanoparticles from bulk material count quantum confinement [22, 23], the surface plasmon effect [24–27], and a high surface-volume ratio [28, 29]. The most commonly used MNPs include noble metals, mainly gold [30–33], silver [34–39], platinum [40, 41], palladium [42–46] and copper [47–50]. Intensive research has been made on strategies to control the shape and size of these materials [24, 51–53].

It is expected that the combination of CNTs and MNPs can generate materials with mixed and even new properties concerning these separate nanostructures, opening an interesting range of applications. In the first methods developed to assembly MNPs and CNTs, nanoparticles were located both on the external surface and inside the nanotube cavity, i.e., non-selectively [54–57] (Fig. 1a). Recently, it has been shown that the physical properties of these nanomaterials

Figure 1 Deposition of metal nanoparticles (MNPs) on carbon nanotubes through non-selective methods leading to random distribution **(a)** and area-selective methods leading to MNPs deposition on the outside of CNTs **(b)**, the inside **(c),** or CNT ends **(d)**.
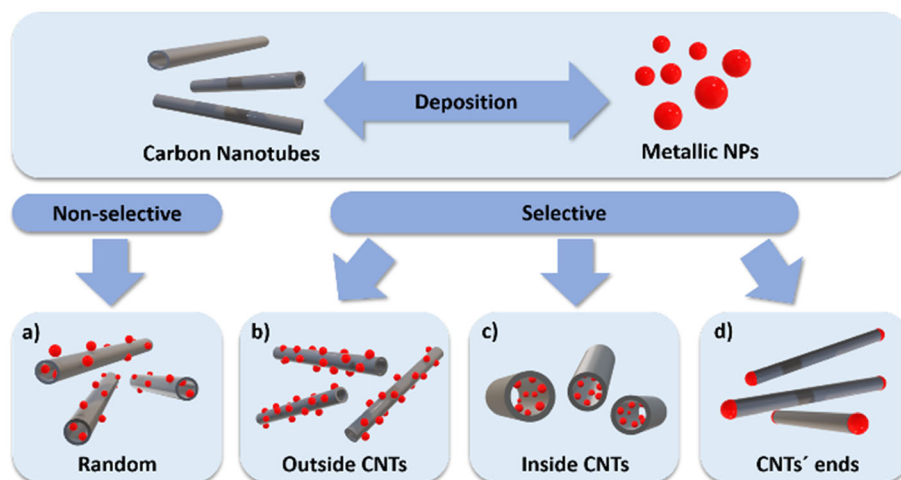
depend on where the MNPs are mainly deposited. This review focuses on three types of area-selective deposition, entailing MNP deposition in (I) the exterior (Fig. 1b), (II) the interior (Fig. 1c), and (III) at the ends of CNTs (Fig. 1d). Selected representative examples are reported in which different methodologies were used to deposit MNPs on CNTs in the three mentioned configurations. The most efficient procedures and the most influential parameters for each method, as well as the characterization techniques that allow corroborating the selectivity of the deposition, will receive special emphasis.

Regarding usefulness, most applications that have been investigated relate to catalysis [58–61]. Using CNTs as support for MNPs has advantages over other substrates like graphite [62], active carbon [63], and silicon dioxide [64]. The promissory reported results show that the use of these hybrid nanomaterials will continue to increase markedly. On the other hand, the properties of these nanomaterials hold promise for use in electronics [65], sensors [66, 67] and biosensors [13, 68], energy conversion and storage devices [69, 70], among others [71–75]. This review summarizes the most effective methods for selectively combining these materials as well as the characteristics necessary for each specific application.

Methods for metal nanoparticles deposition in carbon nanotubes

Several methods exist to couple MNPs and CNTs. Figure 2 contains the most used methods found in the literature, divided into two groups: first, methods in which the formation of the MNPs occurs in the

presence of CNTs (in situ formation), and second ex situ CNT and MNP coupling methods (coupling of previously formed nanostructures).

In situ formation of MNPs in the presence of CNTs

In this group can be distinguished two strategies that differ according to the nature of the nanoparticle formation process. They can be categorized as chemical or physical methods, depending on whether a chemical reaction is involved or not. In both cases, the NP formation process occurs in the presence of CNTs in such a way that the interaction occurs in the early stages of NP growth, acting as a support.

Chemical methods

This group has received the most attention due to the ease of implementation. Salts or molecular compounds are used based on noble metals as synthesis precursors. Methods include aqueous impregnation [76], incipient wetness impregnation [77], precipitation-deposition [78], and electrochemical methods [79, 80]. All these methods have in common a stage of chemical reduction of the precursors for the formation of metal atoms, which subsequently undergo nucleation processes for the formation of the nanoparticle.

Physical methods

These methods generally use bulk metal as precursors. No reaction ensues since the metal is evaporated/atomized under reduced pressure and

Figure 2 Deposition methods employed to prepare CNT-MNP composites.
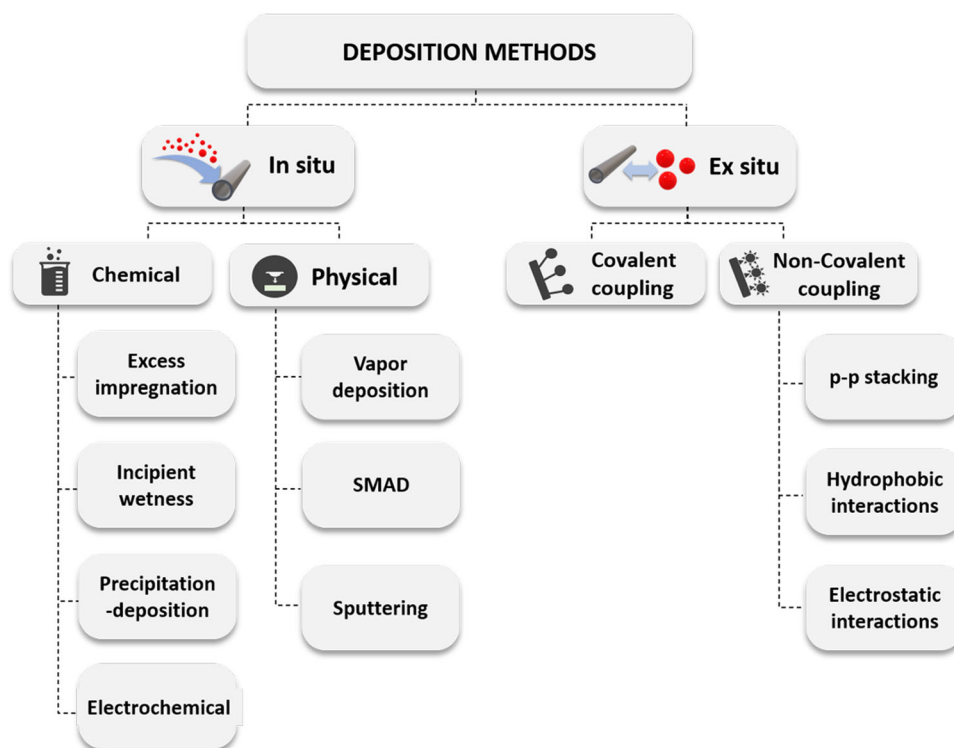
deposited elsewhere with no change of oxidation state, except for reactions that could occur in the interfaces or on the surfaces of nanoparticles. A commonly mentioned method in the literature is physical vapor deposition (PVD) [81, 82]. The method consists of using an electric resistance as a crucible, which is heated until the metal evaporates. Another option to deposit the metal is through cathodic pulverization (sputtering) [83, 84]. Samples prepared through this method have high purity since the metal precursor does not interact with other reagents in the deposition process. The solvated metal atom dispersion (SMAD) method [85] has also been used. It involves the evaporation of the metal in the presence of an organic vapor. Subsequently, the nucleation and growth processes of the nanoparticles occur. In both methods, zero-valent atoms emerge directly from the massive metal, without the need to use a reduction process as with chemical methods.

Coupling of ex situ formed MNPs and CNTs

This classification contemplates the coupling of MNPs to CNTs, both previously formed. Among methods, we can count those that consider the coupling of both nanostructures in a noncovalent way

and those where a covalent union between both nanostructures is promoted.

Noncovalent coupling

In this category, the metal nanoparticles are functionalized with groups that adhere to CNTs via weak intermolecular interactions like p-p stacking [86–90], hydrophobic [91–93], or electrostatic attractions [94–96].

Covalent coupling

In this case, CNTs are covalently modified with organic ligands (linkers) that possess functional groups that allow them to directly coordinate on MNPs' surface (for example, thiols with AuNPs or AgNPs [97–104]). These methods ensure more efficient interaction between both nanostructures [105].

Despite the diversity of methods for preparing these hybrid materials, not all of them are effective in selectively allocating nanoparticles to specific positions. Some methods serve to selectively cover one or the other position, depending on certain CNTs' surface protection strategies. The most common methods for depositing nanoparticles in CNTs are discussed below: first, those that lead to a coating on

Table 1 Overview of works where MNPs have been selectively deposited in the outside walls of CNTs and some of the most relevant parameters used and results obtained in each case

| Reference	Deposition method	CNT internal diameter	CNT external diameter	Oxidation treatment	Metals	% Metal/ Carbon	Solvent	Protective agent	NP size	Selectivity %
Segura 2012 [92]	Noncovalent coupling	–	1,3 nm (SWCNT) 25 nm (MWCNT)	O_2	Au/Pd	–	DMF	–	3 nm (Pd); 7 nm (Au)	~ 100
Tello 2008 [85]	SMAD	–	~ 27 nm	O_2	Au	–	Acetone	–	~ 3,5 nm	~ 100
Scarselli 2012 [81]	Physical evaporation	–	14 – 30 nm	–	Au /Ag / Cu	–	–	–	–	~ 100
Scarselli 2011 [116]	Physical evaporation	5,8 ± 0,3 nm	13,8 ± 0,5 nm	–	Cu	–	–	–	4,6 - 10,2 nm	~ 100
Ajayan 1993 [114]	Physical evaporation	–	–	–	Pb	–	–	–	1–15 nm	~ 100
Guan 2014 [113]	Incipient Wetness	5 – 10 nm	10 – 20 nm	HNO_3	Pd	5%	Acetone	Xylene	~ 5.2 nm	~ 100
Wang 2015 [64]	Incipient Wetness	5 – 10 nm	10 – 20 nm	HNO_3	Pd	< 5%	NH_3 x H_2O	Xylene	3,5 nm	~ 80
Tessonnier 2009 [106]	Incipient Wetness	20 – 50 nm	90 ± 30 nm	HNO_3	Ni	1%	H_2O	Organic solvents	4 – 9 nm	~ 75
Ersen 2007 [77]	Incipient Wetness	15 nm		HNO_3	Pd	10%	H_2O	–	3 – 4 nm	~ 100
Ma 2007 [76]	Aqueous Impregnation	< 10 nm		HNO_3	Pt	~ 3%	H_2O/Ethanol/ 2-propanol	–	< 2 nm	~ 100
Duc Chinh 2019 [117]	Aqueous Impregnation	10 – 20 nm	80 – 100 nm	H_2SO_4/HNO_3 / $HSCH_2CH_2NH_3^+Cl^-$	Au	0.4%	Water	–	15 – 35 nm	–
Xue 2001 [108]	Aqueous Impregnation	–	20 nm	–	Pd / Pt / Au / Ag	< 2%	H_2O/Acetone	–	7/8/8/ 17 nm	~ 100
Gebremariam 2020 [118]	Microwave-assisted Aqueous impregnation	~ 200 nm	–	–	PdAgRu	–	Trisodium citrate/ Ethylene glycol	Water	~ 5 nm	–
Figueira 2018 [112]	Incipient Wetness	14.3 nm	4.6 nm	HNO_3	Co	5%	H_2O	Ethylene glycol	7 nm	–
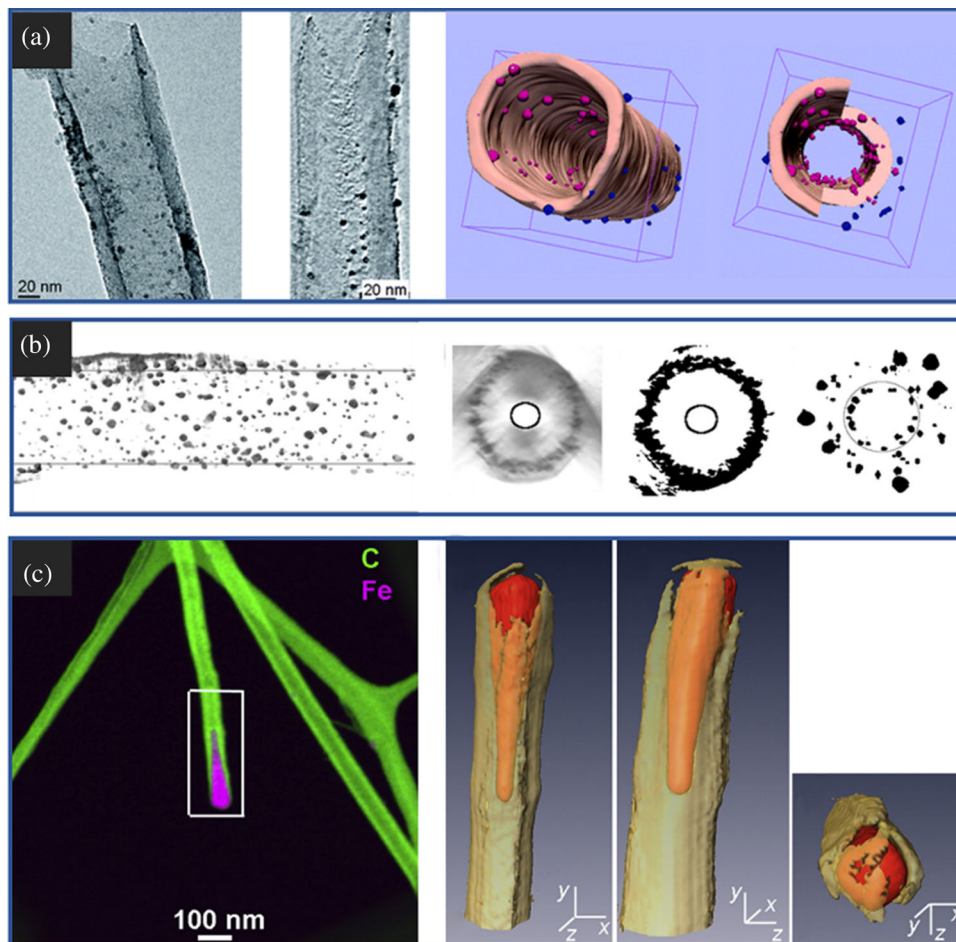
Figure 3 a 2D-TEM image and reconstructed volume of CNT-NiNP composite **(left)** and 3D model **(right)** representing CNTs (pink), NiNPs deposited in the outside of the nanotube (red), and outside the nanotube (blue). (Adapted with permission from Reference [106]. Copyright © 2009, American Chemical Society). **b** 3D models obtained from the reconstructed volume of AuNPs and PdNPs deposited inside CNTs (modified with permission from Reference [77] Copyright © 2007, American Chemical Society). **c** Elemental map of CNT-FeNP composites obtained by EFTEM technique (left) and 3D models built based on the reconstructed volumes (right) showing Fe (red) and C (half-transparent yellow–brown) (modified with permission from Reference, [107] Copyright © 2011, Elsevier B.V.).

the external surface of carbon nanotubes, second in the inner cavity, and third at their ends.

The next section focuses on common characterization techniques that allow demonstrating the selectivity of the hybrid nanostructure preparation methods.

Characterization techniques to evaluate MNPs deposition selectivity in CNTs

The most used characterization techniques to corroborate the location or area of CNTs in which MNPs were deposited are scanning electron microscopy (SEM) and transmission electron microscopy (TEM). Both

techniques allow discovering the morphology of these nanomaterials and identifying the location of the nanoparticles on the internal or external surface, or at the ends of the nanotubes. High-resolution transmission electron microscopy (HRTEM) is used to appreciate more specific details such as nanoparticle geometry and sometimes crystallinity. This technique is also used to estimate the size of the particles and determine the size distribution of the sample. Depending on the preparation method and CNT's characteristics (e.g., internal diameter) or the NPs (e.g., size), it is possible to assert that the NPs will either form or be in a specific sector of nanotubes. However, some authors showed that it is not possible to distinguish the location of the
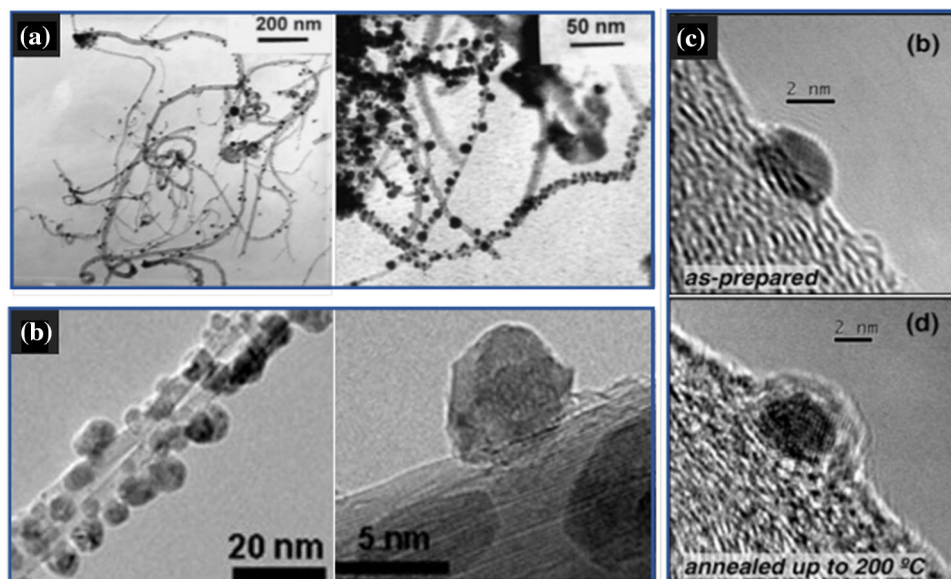
Figure 4 a TEM images of PdNPs (left) and PtNPs (right) deposited in the outside walls of CNTs using a simple chemical impregnation and reduction method (modified with permission from Figs. 1 and 2 in Reference [108]. Copyright © 2001, Royal Society of Chemistry), **b** HRTEM images of CuNPs on the outer surface of CNTs obtained through thermal evaporation of Cu (reprinted with permission from Reference [81]. Copyright © 2011, Elsevier Ltd.) and **c** HRTEM images of AuNPs anchored on CNT walls before (up) and after (below) annealing treatment at 200 °C (reprinted with permission Reference [85], Copyright © 2008, Elsevier Ltd.).

nanoparticles in their entirety from a 2D image; hence, it is not possible to state a deposit selectivity rate. To prove the percentage of nanoparticle deposition inside, outside or at the ends of CNTs, it is necessary to obtain microscopy images from different angles.

It is possible to take TEM images by varying the angle at which the image is generated and then create a 3D model (TEM-3D) to indicate the location of the metal particles and the percentage of those deposited inside or outside of the nanotubes (Fig. 3a) [106]. In this sense, the technique known as Scanning Transmission Electron Microscopy–High Angle Annular Dark Field (STEM-HAADF) is very powerful. Several images with different inclinations are taken, and a 3D model is built based on the 2D images (Fig. 3b) [77]. Also, energy-filtered transmission electron microscopy (EFTEM) is a powerful technique providing not only structural information but also chemical. This way 3D information can be obtained on the morphology but also the chemical nature of the nanocomposite (Fig. 3c) [107]. All these techniques are more efficient to determine the selectivity of each deposition method than conventional TEM and SEM images.

X-ray Photoelectron Spectroscopy (XPS), Energy-Dispersive X-ray Spectroscopy (EDS/EDX), and Electron Energy-Loss Spectroscopy (EELS) are used to complement the data obtained from the above techniques. XPS allows distinguishing the oxidation state of the metal particles and the functional groups present on the carbon nanotubes. EDS and EELS enable conducting an elemental analysis of materials and sometimes generate compositional maps and 3D models with a precision of a few nanometers (Analytical Electron Tomography), which allows discovering the location of the NPs. These techniques, although complementary, are crucial since many times the data obtained can explain the composite properties while using them in any application.

Area-selective deposition of MNPs in CNTs

As stated previously, the methods for preparing these hybrid nanostructures are mostly not specific. However, strategies can be generated that allow increasing selectivity toward the formation of the desired and its corresponding properties Some strategies that have been successful in the formation of specific MNP-CNT composites are discussed in this section.
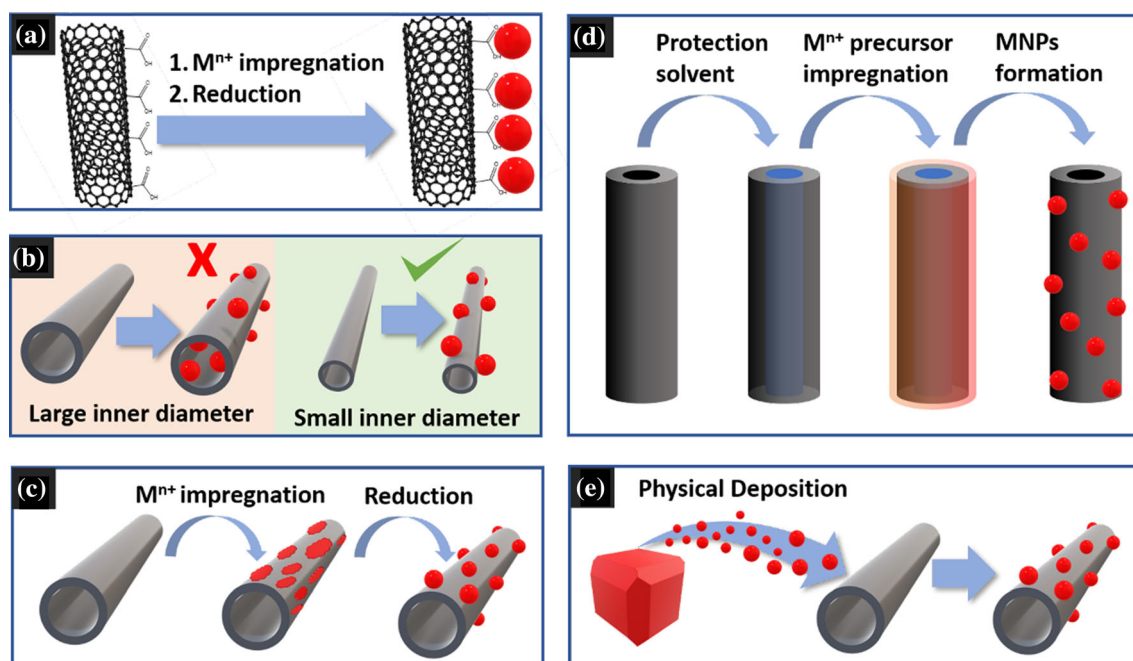
Figure 5 Schematics of some strategies employed to ensure selective deposition of MNPs on the outside of CNTs. **(a)** CNT surface modification with functional groups (COOH in the example), **(b)** incipient wetness method, **(c)** using CNTs with small inner diameter instead CNTs of large inner diameter, **(d)** inner solvent protection strategy, and **(e)** using physical deposition methods such as evaporative deposition.

Selective deposition of MNPs on the external surface of CNTs

Among the most common chemical methods to couple MNPs preferably to the external surface of CNTs count the aqueous impregnation and the incipient wetness methods. Physical methods have also been used, mainly evaporative deposition and less common methods such as SMAD and non-covalent coupling. A description and comparison of some studies in which MNPs were selectively deposited on the external walls of CNTs follow below. At the end of this section, a table summarizing the information of each article is presented, which allows comparing the methods (Table 1).

The aqueous impregnation method comprises impregnating the surface of a support (CNTs in this case) with an excess solution that contains the desired metal precursor salt. Subsequently, the solvent is removed through evaporation, and metal reduction is carried out for the formation of the MNPs. This method has normally been used to deposit low amounts of metal, i.e., < 5% of metal relative to the mass of carbon nanotubes (Table 1). Xue et al. used this method to study the selective deposition of Pd,

Pt, Au, and Ag on the external walls of CNTs (Fig. 4a) [108]. The authors highlighted that when applying ultrasonic treatment, a quantity of the nanoparticles became detached from the nanotubes, suggesting weak adhesion of both nanostructures. This method was also used to deposit Pt nanoparticles on the outer walls of CNTs [76]. Unlike Xue et al. [108], Ma et al. [76] used oxidation treatment on the CNTs before NP deposition. Normally, oxidation treatment involves using HNO_3 (nitric acid) to create functional groups on the surface of the CNTs that contain oxygen (carboxyls, carbonyls, aldehydes, ketones, epoxy groups, among others) and in this way improve MNP adhesion (Fig. 5a). In both cases, the CNTs have a small internal diameter close to 10 nm, which favors the deposition of MNPs on the outer walls (Fig. 5b). In both works it was stated that practically all MNPs were deposited on the external walls of the CNTs. The fact that using CNTs with small internal diameter is an efficient way to ensure that all MNPs are deposited on the external surface of the CNTs, has also been proved in works where SWCNTs are used, since they often have diameters below 2 nm [109, 110]. For example, Asadzadeh et al. used SWCNTs with an internal diameter of ~ 1.5 nm to

Figure 6 Schematics of some strategies developed to selectively deposit MNPs inside CNTs: **(a)** using high inner-diameter CNTs and a solution of MNP precursor in a high surface tension solvent like water, **(b)** impregnating CNTs with the precursor solution followed by using an outer-protective solvent, and **(c)** using CNTs protected in the outside by a solid matrix.
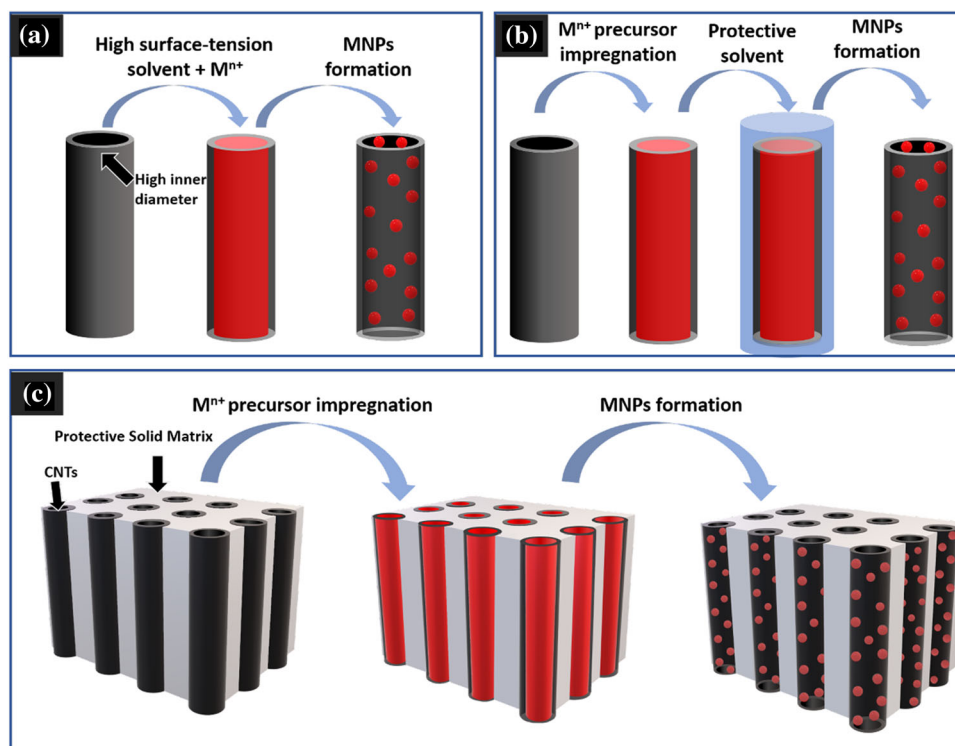
deposit AgNPs with a diameter of ~ 30 nm [111]. They deposited all nanoparticles on the outer walls of the CNTs since the internal diameter is so small that it restricts the characteristic CNT's capillarity phenomenon.

The incipient wetness method has also been widely used (Fig. 5c). This process is similar to the aqueous impregnation method as the three stages of the procedure are the same. Yet in the incipient wetness method, the amount of solution containing the precursor metal salt is much less, since it is only necessary to cover the CNT surface. This way the solution is absorbed mainly into the pores. Unlike classical impregnation, this method allows depositing large amounts of metal ($> 5\%$) concerning the mass of CNTs (Table 1). For example, Ersen et al. reported selective deposition of palladium nanoparticles (PdNPs) on the external walls of CNTs [77]. Due to the deposition of the metal nanoparticles, they carried out an oxidation treatment on the CNTs with HNO_3. They stressed this pre-treatment was essential to improve properties such as surface wettability. The authors wanted to show the influence of CNT internal diameter on the percentage of deposition selectivity, i.e., the amount of MNPs deposited on the outer walls of CNTs in relation to the total deposited MNPs. To achieve this, they compared the deposition

selectivity in nanotubes with an internal diameter of 15 nm and 30 nm from the internal cavity. A 100% selectivity was obtained in the first case, while in the latter it was about 50%.

Another strategy that allows increasing deposition selectivity of MNPs is to use protection agents (Fig. 5d). A protection agent is a physical barrier covering a portion of the nanotubes to avoid the deposition of MNPs at this location. For example, Tessonnier et al. [106] studied a variety of solvents with different percentages of water solubility and boiling points to protect the inner cavity of CNTs with diameters between 20 and 50 nm. As protection agents served octane, ethylbenzene, benzene, trichloromethane, ethylene glycol, N,N-dimethylformamide, ethanol, and tetrahydrofuran (THF). They obtained about 75% deposition selectivity of nickel nanoparticles (NiNPs) on the CNT external walls. More recently, based on Tessonnier's method, Figueira et al. [112] used ethylene glycol as an inner protective agent to deposit CoNPs in the outer surface of CNTs with inner diameters smaller than 10 nm. Interestingly, in this work, CNTs were previously selectively functionalized with Ce and Sr but inside CNTs (see discussion in Sect. 4.2).

Also, Wang et al. [64] studied PdNP deposition using dimethylbenzene as a protection agent for

Table 2 Overview of works where MNPs have been selectively deposited inside CNTs and some of the most relevant parameters used and results obtained in each case

Reference	Deposition method	CNT internal diameter	CNT external diameter	Oxidation treatment	Metals	% Metal / Carbon	Solvent	Protective agent	NP size	Selectivity %
Liu 2014 [78]	Precipitation—deposition	50 – 200 nm	–	–	Pd	1,9%	–	ZnO	2 – 4 nm	~ 100
Segura 2014 [121]	Incipient Wetness	~ 50 nm	~ 70 nm	–	Au	–	2-propanol	AAO membrane	40 nm	~ 100
Guan 2014 [113]	Incipient Wetness	5 -10 nm	10 – 20 nm	HNO$_3$	Pd	5%	Acetone	–	~ 4.9 nm	–
Wang 2015 [64]	Incipient Wetness	5 -10 nm	10 – 20 nm	HNO$_3$	Pd	< 5%	Acetone	–	~ 2,4	~ 80
Hevia 2012 [122]	Incipient Wetness	46 – 29 nm	~ 53 nm	–	Pd	–	H$_2$O/2-propanol	AAO membrane	–	~ 100
Tessonnier 2009 [106]	Incipient Wetness	20 – 50 nm	90 ± 30 nm	HNO$_3$	Ni	1%	Ethanol	H$_2$O	3 – 7 nm	~ 75
Ersen 2007 [77]	Incipient Wetness	30 nm	–	HNO$_3$	Pd	10%	H$_2$O	–	3 – 4 nm	> 50
Ma 2007 [76]	Incipient Wetness	60 – 100 nm	–	HNO$_3$	Pt	3%	H$_2$O/Ethanol/2-propanol	–	~ 5 nm	~ 90
Tessonnier 2005 [63]	Incipient Wetness	–	60 – 100 nm	HNO$_3$	Pd	4,4%	H$_2$O	–	5 ± 1 nm	–
Segura 2014 [121]	Aqueous impregnation	46 nm	~ 53 nm	–	Au	–	2-propanol	AAO membrane	2—10 nm	~ 100
Hevia 2012 [122]	Aqueous impregnation	46 – 29 nm	~ 53 nm	–	Pd	–	H$_2$O/2-propanol	AAO membrane	–	~ 100
Figueira 2018 [112]	Incipient Wetness	14.3 nm	4.6 nm	HNO$_3$	Ce, Sr	7% (Ce) 3% (Sr)	Ethanol	–	2 – 4.5 nm	–
Hajipour 2019 [123]	Aqueous impregnation	5 – 10 nm	20 – 30 nm	HNO$_3$ / H$_2$SO$_4$	Co	0.5%; 5%	H$_2$O	–	21 ± 5 nm; 9 ± 5 nm	~ 100

Figure 7 TEM images of MNP-CNT composites where the MNPs have been selectively deposited inside CNTs: **(a)** PdNPs deposited inside CNTs using an aqueous solution of the precursor and high-diameter CNTs (reprinted with permission from Reference [76]. Copyright © 2007, Elsevier Ltd.), **(b)** NiNPs grown inside CNTs using a protection solvent (reprinted with permission from Reference [106] Copyright © 2009, American Chemical Society), **(c;d)** AuNPs 20 deposited on CNTs using a solid protective matrix and different Au-precursor concentrations (Reprinted from Reference [121] Copyright © 2014, Segura et al.; licensee Springer).
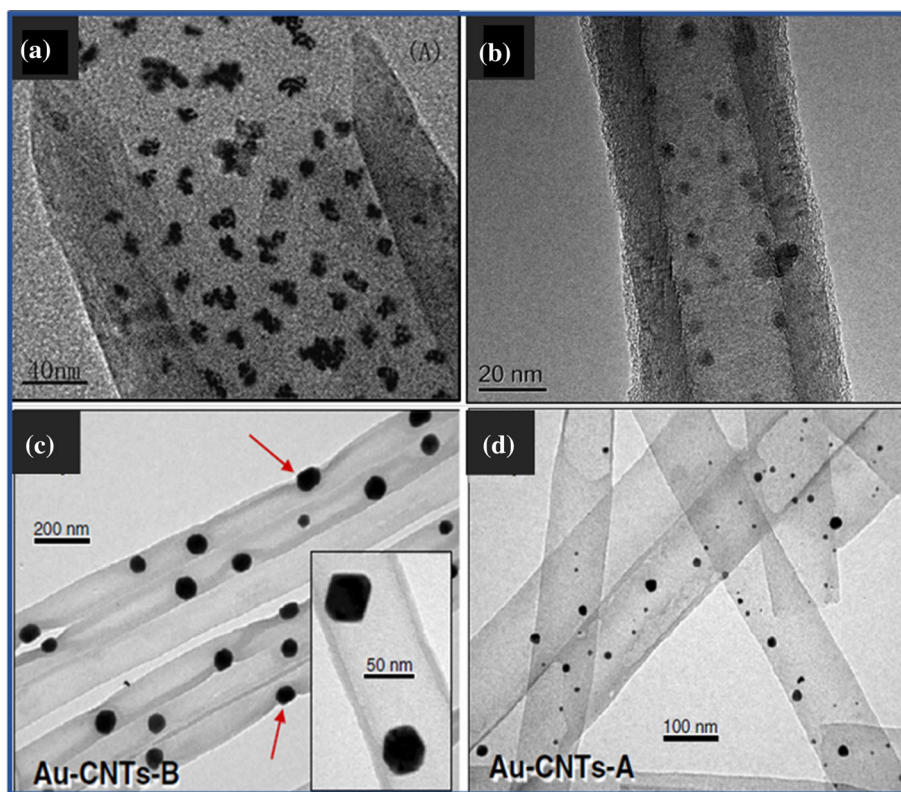
nanotubes with inner diameters between 5 and 10 nm. Around 80% of the PdNPs were deposited on the exterior walls. Also, Guan et al. [113] achieved close to 100% selectivity by also depositing PdNPs on CNTs using a similar approach. In general, the use of solvents as protection agents allows a slight increase in the deposition selectivity percentage.

In sum, the easiest way to deposit the largest number of MNPs on CNT external walls when using the aqueous impregnation and incipient wetness methods is to use MWCNTs with an inner diameter close to or less than 15 nm or use SWCNTs. The smaller the internal diameter, the higher the Van der Waals forces, restricting the capillary phenomenon, which prevents filling the interior of the nanotube.

Regarding physical methods to achieve deposition of MNPs on the outer walls of CNTs, the most common is evaporative deposition (Fig. 5e). For example, Scarselli et al. [81] used thermal evaporation to deposit AuNPs, AgNPs, and CuNPs (Fig. 4b). The authors used a quartz microbalance to monitor the amount of metal as a deposited thickness equivalent. They stated that as the amount of metal evaporated increases, the number of deposited nanoparticles also increases, and they are grouped to form larger NPs.

They also found differences in shape and distribution depending on the metal. The authors concluded that under the evaporative deposition method, the size of the deposited nanoparticles is manageable by varying the amount of evaporated metal.

In general, the evaporation [81, 112, 114] and sputtering [83, 84] methods are the most common ones to deposit MNPs on the external walls of CNTs of any size. Usually ∼ 100% deposition selectivity is obtained. Furthermore, the samples have high purity, since the precursor metal does not need to maintain contact with other reagents during the deposition process. However, a disadvantage of these methods is that deposition occurs directionally on one side of a substrate, forming a film, so that coating of the nanotubes will only occur on its exposed side.

Other physical methods, albeit less common, also exist. Tello et al. [85] used the SMAD technique to deposit AuNPs on MWCNTs (Fig. 4c). They observed that not all deposited particles interacted with the nanotubes. They asserted, however, that the particles that interacted with the nanotubes' wall were firmly anchored to the external surface. Lone et al. [115] also deposited AuNPs but in SWCNTs. They used the spray coating technique which, they highlighted, is

simple and effective for decorating CNTs with MNPs and allowed to obtain particles firmly anchored to the nanotubes' surface.

Selective MNPs deposition inside CNTs

Mainly chemical methods have been used to deposit MNPs in the internal cavity of CNTs. The most used method is incipient wetness and to a lesser extent the aqueous impregnation and precipitation-deposition methods. Table 2 summarizes articles containing these methods. For comparison, the table shows the main parameters of each article presented in this section. Below, the most important aspects of these items are reviewed.

Tessonnier et al. [63] used the incipient wetness impregnation method to deposit PdNPs inside MWCNTs with an external diameter between 60 and 100 nm. They highlighted that most PdNPs were deposited inside the pores, mainly due to the large internal diameter of the pores, allowing the solvent to enter through capillary action, and also because the solvent is water, which allows efficient wetting of the CNT channels (Fig. 6a). This is because water has a surface tension value of 72 mN•m^{-1} [119], and studies have shown that solvents with surface tension under 190 mN m^{-1} are efficient to fill out the CNTs [120]. Other authors have also used water as a solvent to deposit PtNPs in CNTs with an even larger internal diameter. Ma et al. [76] reported about 90% filling efficiency for CNTs with diameters between 60 and 100 nm (Fig. 7a), while Ersen et al. [77] could deposit only just over 50% of PdNPs in the CNT channels using nanotubes with an internal diameter of approximately 30 nm, despite in both works the same solvent was used. Hence, it becomes clear the influence of CNT pore diameter: the greater the internal

diameter of the nanotube, the more MNPs will be deposited inside.

Figueira et al. [112] developed an incipient wetness method based on Tessonnier's results to synthesize Ce and Sr NPs inside CNTs with a very small inner diameter (< 10 nm). They also reproduced Tessonnier's results for NiNPs. Nevertheless, even when they were able to prepare NPs inside CNTs, a lack of selectivity was found due to the small inner diameter of the CNTs.

Wang et al. [64] analyzed the effect of the CNT inner diameter, using acetone as the solvent for PdNP deposition. They found that for a 5% metal charge, 71% of PdNPs formed inside the pores when the inner diameter was 5 nm to 10 nm, while the deposition percentage was close to 80% when the diameter was 20 nm to 50 nm. They also incorporated other studies that allowed analyzing the influence of different parameters that can generate variations in method selectivity. They analyzed the effect of pre-oxidation treatment that is normally carried out on CNTs and found that fewer PdNPs were deposited on the external walls of CNTs without pre-oxidation treatment. On the other hand, when analyzing the effect of the precursor concentration, they noted that 90% of PdNPs were deposited inside the CNTs with 2.5% metal load, while only 80% of the PdNPs were deposited inside the pores when the metal was up to 5%. Hence, when the precursor solution has a higher concentration of metal ions, more MNPs are deposited on the external walls of the CNTs. Other authors used the same solvent to deposit PdNPs inside CNTs with diameters between 5 and 10 nm [113]. NPs deposited within the pores reached an average size close to 5 nm, i.e., only slightly smaller than the size of the cavity. With this, the authors noted that the

Table 3 Overview of works where MNPs have been selectively anchored at CNT ends and some of the most relevant parameters used and results obtained in each case

| Reference	Deposition method	CNT internal diameter	CNT external diameter	Oxidation treatment	NPs	NP Precursor	NP size
Zhao 2013; 2015 [124, 125]	Incubation–reduction	30 nm	–	HNO$_3$/H$_2$SO$_4$	Au	HAuCl$_4$	$\sim$ 30 nm
Segura 2006 [127]	Chemical Vapor Deposition	7.6 nm	38 nm	–	Fe	FePC	$\sim$ 30 nm
Abrams 2007 [129]	Chemical Vapor Deposition	5–20 nm	$\sim$ 35 nm	–	Fe, Cu	Ferrocene, Cu metallocene, Fe$_2$(NO$_3$), Cu$_4$(NO$_3$)$_2$	$\sim$ 15–25 nm
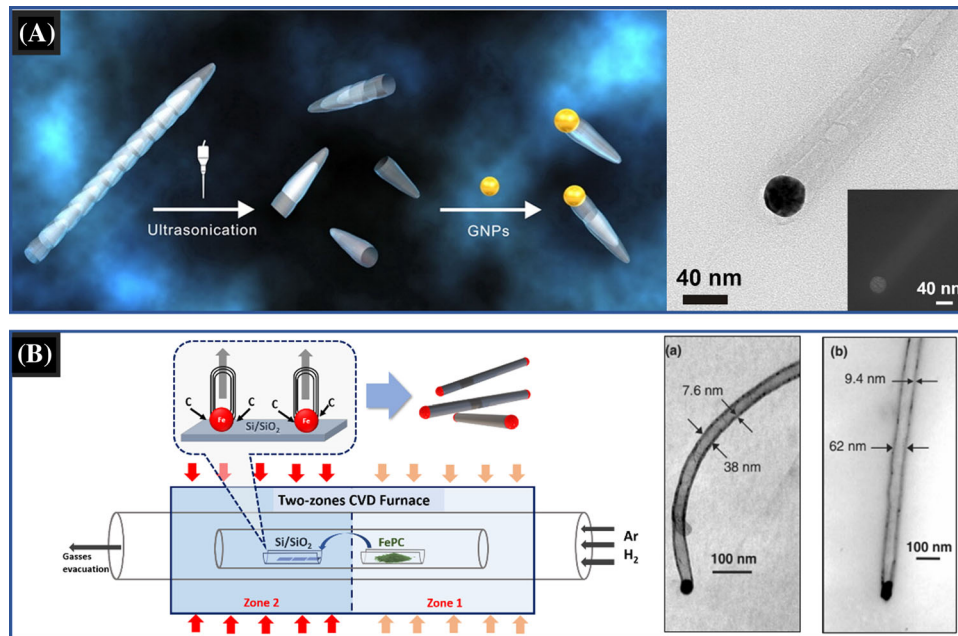
Figure 8 Schematics of strategies to obtain MNPs anchored at the ends of CNTs **(left)** and TEM images of the as-obtained MNP-CNT composites **(right)**: **(a)** using a covalent coupling method between carbon nanotubes cups and AuNPs and **(b)** by iron phthalocyanine catalytic decomposition where Fe nuclei are formed and CNTs are grown from them to obtain FeNPs anchored at the end of the CNTs. (a) Reprinted with permission from Reference [126] (Copyright © 2012, American Chemical Society) and (b) from Reference [127] (Copyright © 2006, American Scientific Publishers).

CNT internal diameter also limits the size of the NPs that are formed.

As in selective deposition in the exterior via aqueous impregnation, some researchers have used solvents as protection agents to ensure that MNPs are formed only inside the pores (Fig. 6b). An example is the deposition of nickel nanoparticles (NiNPs) inside CNTs, using water to protect the surface (Fig. 7b) [106]. In this case, they use just the necessary metal precursor solution amount to fill the interior volume of the nanotubes. Thus, the protection agent (water), having a surface tension greater than that of the solvent of the precursor solution (ethanol), protects the filled pores, ensuring the metal solution is kept inside. Through this method, a 75% efficiency was obtained, considerably higher compared to the classical impregnation method with an efficiency close to 50%.

Solid-state protection agents have also been used (Fig. 6c). In a work developed by our research group [122], CNTs were synthesized using an anodized aluminum oxide (AAO) membrane as a template. Once CNTs had grown, the membrane served to protect their external surface and facilitated the

PdNP selective deposition inside the tubes. For the deposition of nanoparticles, we used the incipient wetness and aqueous impregnation methods. Comparing both, we identified a much higher amount of deposited metal in the form of PdNPs under the incipient wetness method. Samples prepared under the aqueous impregnation method were loaded with much fewer NPs. This work also included an analysis of the influence of the metal precursor salt used for the growth of PdNPs. We studied the number of NPs deposited via aqueous impregnation when using $PdCl_2$ and $Pd(NO_3)_2$ as metal precursors. It emerged that the $PdCl_2$ precursor allows a much higher deposition efficiency. This phenomenon is associated with the formation of the soluble metal complex ion $[PdCl_4]^{2-}$, which could penetrate the pores more easily than the precursor $Pd(NO_3)_2$ and precipitates in dissolution. Similar work was also published by our group, where AuNPs were grown inside CNTs. Herein, it was studied the effect of the precursor salt concentration on the size of the AuNPs formed [121]. Using 1 M solution, AuNPs of 40 nm in diameter were obtained (Fig. 7c), while with a 0.001 M solution

the nanoparticles had diameters of between 2 and 10 nm (Fig. 7d).

Selective MNP deposition at the ends of CNTs

The deposition of MNPs at the exteriors of CNTs is less addressed in the literature because it is complex to get the metal nanoparticles to form or couple only at the ends of the pores and not on the rest of the surface. However, there are high expectations for the use of these materials in electronic and biomedical applications. Table 3 summarizes some of the most relevant articles and parameters that have been used to achieve selective deposition of MNPs at the ends of the CNTs.

One interesting strategy relies on corked carbon nanotubes cups. To achieve this, carbon nanotubes with the bamboo-like structure are prepared, which consists of several attached carbon nano-cups (CNCs) that can be individualized by ultrasonic treatment [124]. These CNTs possess a closed ending in one of the tube's axes and an open one in the other extreme of the tube. So on, it is interesting to place a metal nanoparticle in the open tip forming a nanocomposite where the MNP corks the end of the tube. These kinds of nanocomposites are very promising as selective drug carriers [125].

Zhao et al. have prepared this kind of materials in situ by incubating nitrogen-doped carbon nano-cups (NCNCs) in an AuCl$_4$ solution, followed by a reduction procedure with trisodium citrate at 70 °C [124, 125]. The NCNCs-AuNPs are further separated by ultracentrifugation. TEM images of the composites show the formation of AuNPs at the open end of the cup, due to the major presence in this area of functional groups that anchor Au nuclei on their formation. Nevertheless, some small Au clusters (< 1 nm diameter) can be found in the external face of NCNCs.

Zhao et al. have also developed ex situ coupling methods to achieve NCNCs-AuNPs composites [126]. In this case, NCNCs are fabricated by CVD, followed by ultrasonication procedures (Fig. 8a, right), and their surface is modified with thiolated molecules to favor their covalent coupling to AuNPs. TEM images of this composites are shown in Fig. 8a, extreme left.

Another way to ensure that NPs are selectively located at one end of the CNTs is during the CNT synthesis process. In catalytic CVD methods, for example, CNTs grow from MNPs of some metals such as Fe, Ni, Co, Pd (among others) acting as growth seeds. If the interaction generated between the growth substrate and the MNPs is not too strong, when the CNTs are released from the surface they become attached to the nanoparticle from which they grew (located at one end of the CNTs). For example, we have prepared MWCNTs using iron (II) phthalocyanine, which act as catalyst and carbon source simultaneously. In iron (II) phthalocyanine pyrolysis, FeNPs are formed in situ and serve as growth nuclei for MWCNTs, which are loosely tied to the substrates and walls of the CVD reactor (Fig. 8b). By removing these MWCNTs, the FeNPs become anchored at one end of the CNTs [127], giving magnetic characteristics to these hybrid nanostructures [128].

Abrams et al. also used a similar procedure to prepare copper-tipped carbon nanotubes. In this case, several catalysts consisting of a mixture of copper and iron composes (such as metallocenes, nitrates, and oxides) and CVD procedures were performed using acetylene as a carbon precursor. Bamboo-like nanotubes were obtained, containing Fe-CuNPs in the tips of the open tubes [129].

Applications of MNPs selectively supported in CNTs

The physical and chemical properties of hybrid MNP-CNT nanostructures vary depending on the location of the nanoparticles. This mainly happens because of the differences in the physicochemical environment generated in each case. For example, diffusion processes outside the CNT are different from those in the confined space of the CNT pore [130]. Changes also occur in the electronic distribution of the graphitic mesh due to the curvature of the tube, which modifies the interaction with the NPs [131]. These and other effects could occur in different locations (in, out, end). Therefore, the variation in the properties of these materials directly influences their application.

Considering that most studies involve selective deposition of noble metal NPs in CNTs, it is consistent that the most addressed application points out heterogeneous catalysis [132, 133]. In this sense, significant differences have been found regarding catalytic activity depending on the location of MNPs in

CNTs [130, 132, 134, 135]. Specific examples are further discussed in the next subsection.

Also, some reports showed that these composites, with selectively positioned MNPs, could find use in hydrogen storage [136, 137] and detection [138, 139], or optical and electronic applications. For magnetic applications relatively large magnetic MNPs are used, while small particles deposited in the internal cavity of the CNTs will be essential to adjust the electromagnetic properties and serve in dielectric or shielding applications [140, 141]. Finally, some reports have been published analyzing some properties of these materials to tentatively demonstrate that they could be useful in some of the fields already mentioned. In the next sub-section, description and analysis are given on how the location of the nanoparticles affects certain applications addressed in the literature.

Heterogeneous catalysis

In catalysis, a widely discussed research topic is the selective hydrogenation of organic compounds. An example is the selective hydrogenation of commercially crucial cinnamaldehyde (CALD). From the hydrogenation of CALD, it is possible to obtain as products hydrocinnamaldehyde (HCALD), cinnamic alcohol (CA), and phenyl propanol (PP). Of these products, one of the most sought-after is CA for its use in the perfume industry, both for its aroma and its fixing properties. It is also used in the synthesis of chloromycetin antibiotics. Also, HCALD is used as an intermediary in the synthesis of drugs to treat HIV [63, 76, 142].

Ma et al. [76] studied the hydrogenation of CALD to CA from the comparison of catalysts composed of platinum particles deposited inside (Pt/CNT-in) and outside (Pt/CNT-out) of carbon nanotubes and observed significant differences. In the catalytic tests carried out with Pt/CNT-in, it was observed that 60% of the product was CA, while with Pt/CNT-out only 10% of CA was obtained. In this case, the nanotubes of the Pt/CNT-in catalyst had an internal diameter of 60 nm to 100 nm and the CNTs of the Pt/CNT-out catalyst of less than 10 nm. Consistently, the PtNPs deposited in the Pt/CNT-in catalyst are larger (5 nm) than in the Pt/CNT-out catalyst (2 nm). The authors indicated that the main selectivity factor in this case was MNP size. Some authors reported that as particle size increased, selectivity for CA formation increased

[143, 144]. The larger the metal surface in contact with the CNT wall, the better the transfer of π electrons that occurs from the graphitic planes to the metal particle [145]. Consequently, the charge density in the metal increases, and the CALD molecule generates a repulsion between the phenyl ring and the metal surface, protecting the nearby C = C bonds. In this sense, the role of CNTs is fundamental, since their internal and external diameter allows modulating the size of the particles that grow on their surface. Tessonnier et al. [63] also reported a material like the Pt/CNT-in catalyst prepared by Ma. In both cases, the metal particles were 5 nm in size and the carbon nanotubes were between 60 and 100 nm in diameter. However, Tessonnier et al. used particles of a different metal (PdNPs). The results showed that the catalyst composed of PdNPs deposited inside CNTs was highly efficient in the formation of HCALD, obtaining an 80% yield, and did practically not form CA, highlighting the importance of metallic nature. Some authors have highlighted that the metals of the first transition series favor HCALD formation, while those of the third series favor CA formation [146–148]. Therefore, by knowing the characteristics of the material such as the majority location of the particles in the CNTs and the metallic nature, it is possible to predict the products that will be obtained, which is a significant advance in the petrochemical and fine chemical industry.

Another reaction of great importance for the petrochemical industry is the hydrogenation of CO_2 to methanol. Wang et al. [64] studied this reaction using two catalysts (Pd/CNT-in and Pd/CNT-out). The catalytic activities of these materials were compared with two catalysts prepared with the same metal nanoparticles using silicon dioxide (SiO_2) and activated carbon (AC) instead of CNTs. This time, the Pd/CNT-in catalyst led to much higher amounts of methanol than the other three catalysts. The number of methanol molecules produced per Pd site exposed per hour, known as turnover frequency (TOF), was used to compare the activity of the four catalysts. Pd/CNT-in catalyst's TOF was 3.7 times higher than the Pd/CNT-out catalyst, 3.0 times higher than Pd/AC, and 5.5 times higher than Pd/SiO_2. The authors reported that in the formation of methanol, H_2 and CO_2 activation were fundamental processes. Palladium can activate the H_2 molecule easily; however, it has low catalytic activity for the formation of methanol, so the limitation must be found in the

activation of CO_2. With this argument, the authors explained that the Pd/CNT-in catalyst presents a superior catalytic activity in comparison with the other catalysts. The different surface chemistry between the external and internal walls of the CNTs influences the oxidation state of the PdNPs. XPS analyses of the catalysts showed a marked difference in the percentage of different palladium species. In the case of the Pd/CNT-out catalyst, 47.6% of Pd^0, 47.8% of Pd^{2+}, and 4.6% of Pd^{4+} were observed. Meanwhile, in the Pd/CNT-in catalyst, 13.8% of Pd^0, 74.6% Pd^{2+}, and 11.6% Pd^{4+} were observed. It is possible that when the PdNPs are covered by the walls of the CNTs, in the reduction stage, they are protected and cannot be completely reduced. This fact suggests that the $Pd^{\delta+}$ species activate the CO_2 molecules, favoring the formation of methanol in comparison with the other catalysts.

Guan et al. [113] reported enantioselective hydrogenation of carboxylic α,β-unsaturated acids using the Pd/CNT-in, Pd/CNT-out, and Pd/AC catalysts. As a result, they found that the Pd catalyst within the channels of the CNTs shows higher activity and enantioselectivity than the other two catalysts, leading to results that showed enantioselectivity close to 92%. The authors also reported enantioselective hydrogenation of α-ketoesters using PtNPs encapsulated inside CNTs and distributed outside. Results showed that the Pt/CNTs-in catalyst's performance was much higher than the Pt/CNT-out catalyst and even the Pt/Al_2O_3 catalyst, also used for the comparison.

Energy conversion and storage

The selective coupling of MNPs and CNTs holds much promise to be useful in energy production and storage. With the inevitable transition from a fossil fuel-based economy to a clean and sustainable energy economy, manufacturing high-efficiency, low-cost energy storage devices is currently a critical area of research globally. The most promising alternatives at present are devices for solar-driven water splitting [149, 150], photovoltaic cells [151, 152], and metal-air batteries [153, 154]. A key limiting process on many of these devices is the oxygen evolution reaction (OER), which slow kinetics at low temperatures requires large overpotentials to drive the four-electron oxidation process [155–157]. Until now, RuO_2 and IrO_2 are the reference OER catalysts, but their high cost and scarcity considerably limit their application on a large scale [155, 158, 159]. Therefore, low-cost, efficient, and durable non-precious metal OER catalysts such as Fe, Ni, and Co have received much attention recently [159–162].

In this sense, the combination of OER catalysts to carbon nanotubes has also come into focus as a very promising strategy. For example, Liu et al. [163] formed nanoparticle hybrids of these three non-precious metals (FeNPs, NiNPs, and CoNPs) with nitrogen-doped CNTs (NCNTs). In all composites, the MNPs were deposited inside CNTs. The Co@NCNT, Fe@NCNT, and Ni@NCNT catalysts achieved a current density of 10 mA cm^{-2} with an overpotential of 0.39 V, 0.52 V, and 0.59 V vs. RHE, respectively, in 0.1 M KOH alkaline solution. The authors highlighted that the overpotential value of the Co@NCNT catalyst is close to the value of the RuO_2 reference catalyst with an overpotential of 0.37 V at 10 mA cm^{-2}. It is generally significant to compare the overpotential values to achieve a current density of 10 mA cm^{-2} since it is a relevant value in the synthesis of solar fuel [164, 165]. Yu et al. [166] also used MNPs deposited inside NCNTs to study the OER. In this case, they used a nickel–cobalt alloy forming NiCo@NCNT hybrids and compared it to individual Ni@NCNT, Co@NCNT, and IrO_2 metal hybrids as the reference catalyst. The overpotentials to achieve a current density of 10 mA cm^{-2} were 0.41 V, 0.45 V, 0.45 V, and 0.46 V for NiCo@NCNT, Ni@NCNT, IrO_2, and Co@NCNT, respectively. The NiCo@NCNT hybrids, besides having a lower potential than IrO_2, were more stable after performing 1,000 cycles of OER in 0.1 M KOH medium, which suggests the superiority of encapsulation of MNPs in NCNTs. It was also found that enveloped MNPs effectively resisted exposure to hostile chemical environments because of protection by carbon layers, leading to high stability.

Hou et al. [167] produced hybrid 3D NiCoNPs deposited at the ends of NCNTs grown in porous carbon nanosheets doped with N (NPCN). The NPCN-NiCo@NCNTs hybrids provided surprising results for the OER by presenting a current density of 10 mA cm^{-2} at 1.59 V. The authors highlighted that these results were better than those obtained by the commercial Ir/C catalyst (1.62 V), and comparable with the non-precious catalysts previously reported as IrO_2 (1.68 V), RuO_2 (1.59 V), $Mn_3O_4/CoSe_2$ (1.68 V), Co_3O_4/N-graphene (1.54 V), all in alkaline

medium (0.1 M KOH). They also studied the catalytic activity of these hybrids in the oxygen reduction reaction (ORR), which is also essential for achieving high efficiency in energy production and storage. The NPCN-NiCo@NCNT composites showed a current density of 26.4 mA cm^{-2} at 0.8 V. This result was compared with the commercial Pd/C (18.6 mA cm^{-2}), NPCN (17.2 mA cm^{-2}), NiCo@NCNT (6.1 mA cm^{-2}) catalysts, which confirmed the excellent performance for ORR of the fabricated hybrid material. The results for OER and ORR demonstrate the advantages of fabricating 3D nanostructures. The strategic position of the NiCoNPs coupled at the ends of the nanotubes improves the activity of the catalyst, while the NPCN allows easy access to the active sites because it acts as a template and allows the ordered growth of NiCo@NCNT structures. NiCo@NCNT structures have superior electrical conductivity, which could facilitate electron transport during electrocatalysis, which is supported by the much lower interfacial charge transfer resistance results of NPCN-NiCo@NCNT compared to NPCN because of the introduction of NiCo@NCNT.

Other applications

Much research in biomedicine is related to biosensors for the early detection of catastrophic diseases [13]. Asadzadeh et al. [111] used AgNPs deposited on SWCNT external walls as an electrochemical micro-RNA (miRNA) marker. Selective detection with high sensitivity of miRNAs is of great importance because these non-coding single-stranded RNA strands regulate the translation of specific genes' encoding proteins. The unusual expression of miRNA is directly associated with various catastrophic diseases such as diabetes, cancer, cardiovascular disease, and neurological disorders. In this work, two parallel studies were carried out. First, the authors tested if a difference existed in the binding of Ag@SWCNT hybrids to single and double-stranded nucleic acids, considering that SWCNTs interact with nitrogenous bases through π-π interaction, while AgNPs produce electroanalytical signals facilitating system monitoring. The results indicated that the prepared electrochemical marker has a high affinity for binding to single-stranded DNA (ssDNA); however, π-π interaction with double-stranded DNA (dsDNA) is weaker because the nitrogenous bases were protected by

forming the double helix. This difference in the results using AgNP/SWCNT as an electrochemical marker showed that a simple method can detect the nature of (single and double-stranded) nucleic acids. The second study was to verify the usefulness of the proposed nanogenosensor for which they analyzed the detection of miR-25, a known biomarker of real blood plasma lung cancer samples. The authors showed that precise oxidation peaks corresponding to the binding of Ag@SWCNT nanohybrids to nucleic acids that were not anchored to the miR-25 biomarker were observed in all electrochemical tests performed on real samples. They also highlighted that if some experimental conditions were optimized, it would be possible to monitor miR-25 in the clinical stage.

Another application of significant interest is the production of new polymeric compounds with electromagnetic properties. In this sense, it is important to exploit the simultaneous properties of nanohybrids, such as the electrical transport of CNTs and the magnetism of MNPs. For example, Andreev et al. [141] deposited CoNPs inside MWCNTs forming ferromagnetic nanohybrids that were used to form a polymeric composite with polyethylene (PE). The authors emphasized the importance of being able to protect the CoNPs with the wall of the MWCNTs since conventional techniques for synthesizing composite materials such as mechanical mixing or suspension in a molten polymer are inappropriate to introduce highly pyrophoric materials such as CoNPs [140]. Additionally, the unexpected ferromagnetism of these small nanoparticles was attributed to the formation of high aspect ratio structures by the effect of the tubular cavity of the MWCNTs. The polymerization was performed in situ directly in the Co@MWCNT nanohybrid, and pure MWCNTs for comparison. Conductivity measurements were then carried out to the PE polymer alloyed with the Co@MWCNTs hybrid nanostructures, and it was compared to the PE-MWCNT composite. They found that conductivity improved by an order of magnitude in the composite Co@MWCNT-PE) compared to the composite without CoNPs, and also found that CoNPs encapsulated in the MWCNTs resisted sintering up to 550 °C, among other qualities This proved that the combination of these materials is a promising option for the generation of new multifunctional composites.

Wen et al. [168] also prepared composite materials of Co@CNT, Ni@CNT, and Fe@CNT dispersed in

epoxy resin, where the MNPs were previously deposited in the internal cavity of the CNTs. These compounds exhibited excellent microwave absorption properties in the S-band due to an appropriate combination of the complex permeability and permittivity values resulting from magnetic NPs and the lightweight of CNTs. The best results were obtained with the Fe@CNT absorber. The authors concluded that this is a promising candidate for potential use in electronic and communication devices that use the 1–40 GHz electromagnetic waves range like microwave black boxes, Wi-Fi networks, and fixed satellites.

Conclusions

In the present review, it has been possible to identify the key methods and parameters that allow the area-selective deposition of MNPs on CNTs in three configurations: MNP decoration on the outside, inside, and at the ends of CNTs.

To deposit MNPs on the external walls of CNTs, it has been demonstrated that various chemical and physical methods can be used allowing the obtention of high selectivity percentages. However, the most efficient in terms of selectivity are physical methods, being the evaporation deposition the most used of them. Less used methods that allow depositing all MNPs on the exterior walls also exist, for example: SMAD, sputtering, and spray coating. Furthermore, samples prepared with these techniques have high purity. Although of easy implementation, chemical impregnation methods are somewhat less selective because the precursor ions diffuse through the CNT external and internal surfaces. Hence, different strategies to achieve high selectivity percentages must be employed. For impregnation methods, the simplest form to achieve a high selectivity in the outside deposition is using MWCNTs with an internal diameter smaller than or close to 10 nm or using SWCNTs with less than 2 nm in diameter. On the other hand, using solvents as protective agents allows to increase selectivity, but does not ensure that all MNPs are deposited on the exterior walls of the CNTs. Coupling preformed MNPs to CNTs is the most demanding technique, since several stages are needed, including the formation of MNPs, chemical modification of the materials, and coupling procedures. However, due to the large volume of ligands

that bind to nanoparticles, the probability that deposition occurs only on the outer walls is very high.

Chemical impregnation methods have been the most used to deposit MNPs inside CNTs. Conventional impregnation methods have proved to be inefficient in allowing all particles to lodge inside the nanotube's cavity. That is why some strategies have been developed to achieve selective deposition. Under the aqueous impregnation method, it is necessary to use CNTs with a diameter close to or greater than 30 nm, since otherwise, very low metal deposition percentages are obtained. This behavior contrasts with the incipient wetness method which allows nanotubes with a small internal diameter $\sim$ 10 nm to be used and still deposit MNPs inside. To our knowledge, the only strategy that currently allows for selectivity percentages of inner deposition close to 100% is the use of physical protection agents. However, filling efficiency will vary depending on the impregnation method and metal precursor employed. The incipient wetness method has a higher filling efficiency than the aqueous impregnation method. At the same time, the size of the NPs formed can be much larger depending on concentration, and CNT inner diameter, this last constitutes a growth limit.

Regarding the deposition of MNPs at the ends of CNTs, carbon nanotubes in the form of nano-cups have been used to ensure the formation of MNPs on the open-ended tip. Also, by controlling chemical vapor deposition conditions and using MNPs as a catalyst for CNTs growth, it can be ensured the formation of MNPs-ended CNTs. Articles found do not specifically focus on the percentage of selectivity. Importantly, this type of coupling is the least common in the literature.

To corroborate the area selectivity in the deposition of MNPs in CNTs, it is necessary to use electron microscopy techniques. The most used are SEM and TEM since both allow a general identification of nanoparticle locations in CNTs. However, some authors indicate that from a 2D image, it is not possible to distinguish the location of the MNPs with complete certainty. Therefore, it is necessary to take a series of microscopy images from different angles. This allows generating of 3D models to corroborate both the location of the MNPs and the percentage of filling either inside, outside or at the ends of the

CNTs. These techniques include TEM 3D and STEM-HAADF.

The area-selective deposition of MNPs on CNTs, in the three studied configurations, has been widely used in heterogeneous catalysis in many crucial reactions in fine chemistry and petrochemicals. On the other hand, they have gained importance in the manufacture of high-efficiency and low-cost energy storage and conversion devices, including solar cells, metal-air batteries, and devices for solar-driven water splitting. Great expectations have emerged for its use in biomedical applications as contrast agents in magnetic resonance imaging, treatment mediators, cancer sensors, and manufacturing compound nanomaterials for the formation of polymers with new electro-magnetic properties.

Using CNTs as support for MNPs has definite advantages over the most used supports such as graphite, activated carbon, and silicon dioxide, among others. However, it is necessary to gain a comprehensive view regarding the most effective methods to couple these materials with the characteristics determined for each specific application, which has been the primary reason for this review.

Acknowledgements

Declarations

Conflicts of interest The authors declare that they have no known competing financial interests or personal relationships that could have appeared to influence the work reported in this paper.

References

[1] Ibrahim KS (2013) Carbon nanotubes-properties and applications: a review. Carbon Lett 14:131–144. https://doi.org/10.5714/CL.2013.14.3.131

[2] Popov VN (2004) Carbon nanotubes: properties and application. Mater Sci Eng R Reports 43:61–102. https://doi.org/10.1016/j.mser.2003.10.001

[3] Anzar N, Hasan R, Tyagi M et al (2020) Carbon nanotube - a review on synthesis, properties and Plethora of applications in the field of biomedical science. Sensors Int 1:100003. https://doi.org/10.1016/j.sintl.2020.100003

[4] Mohammad Nejad S, Srivastava R, Bellussi FM et al (2021) Nanoscale thermal properties of carbon nanotubes/ epoxy composites by atomistic simulations. Int J Therm Sci 159:106588. https://doi.org/10.1016/j.ijthermalsci.2020.106588

[5] Pełech I, Pełech R, Narkiewicz U et al (2020) Magnetic and electrical properties of carbon nanotube/epoxy composites. Mater Sci Eng B Solid-State Mater Adv Technol 254:114507. https://doi.org/10.1016/j.mseb.2020.114507

[6] Kumar SD, Ravichandran M, Alagarsamy SV et al (2020) Processing and properties of carbon nanotube reinforced composites: a review. Mater Today Proc 27:1152–1156. https://doi.org/10.1016/j.matpr.2020.02.006

[7] Teixeira-Santos R, Gomes M, Gomes LC, Mergulhão FJ (2021) Antimicrobial and anti-adhesive properties of carbon nanotube-based surfaces for medical applications: a systematic review. Science 24:102001. https://doi.org/10.1016/j.isci.2020.102001

[8] Kumanek B, Janas D (2019) Thermal conductivity of carbon nanotube networks: a review. J Mater Sci 54:7397–7427. https://doi.org/10.1007/s10853-019-03368-0

[9] Monthioux M, Kuznetsov VL (2006) Who should be given the credit for the discovery of carbon nanotubes? Carbon N Y 44:1621–1623. https://doi.org/10.1016/j.carbon.2006.03.019

[10] Wiles PG, Abrahamson J (1978) Carbon fibre layers on arc electrodes-I. their properties and cool-down behaviour. Carbon N Y 16:341–349. https://doi.org/10.1016/0008-6223(78)90072-6

[11] Oberlin A, Endo M, Koyama T (1976) Filamentous growth of carbon through benzene decomposition. J Cryst Growth 32:335–349. https://doi.org/10.1016/0022-0248(76)90115-9

[12] Iijima S (1991) Helical microtubules of graphitic carbon. Nature 354:56–58. https://doi.org/10.1038/354056a0

[13] Zhu Z (2017) An Overview of Carbon Nanotubes and Graphene for Biosensing Applications. Nano-Micro Lett 9:1–24. https://doi.org/10.1007/s40820-017-0128-6

[14] Racca L, Cauda V (2021) Remotely activated nanoparticles for anticancer therapy. Nano-Micro Lett 13:11. https://doi.org/10.1007/s40820-020-00537-8

[15] Zhang T, He J, Xie W, Sun C (2020) Plasmonic properties of a honeycomb structure formed by metallic nanoparticles. Phys E Low-dimens. Syst Nanostruct. 118:113901. https://doi.org/10.1016/j.physe.2019.113901

[16] Alshakhanbeh MA, Ahmed MA, Abou-Gamra ZM, Madien H (2020) Influence of dispersion of various proportions of metallic gold nanoparticles on the optical and photocatalytic properties of titania. Mater Sci Energy Technol. 3(429):439. https://doi.org/10.1016/j.mset.2020.02.007

[17] Dhull N, Nidhi GV, Tomar M (2019) Antimicrobial properties of metallic nanoparticles: a qualitative analysis. Mater Today Proc 17:155–160. https://doi.org/10.1016/j.matpr.2019.06.413

[18] Chen M, He Y, Wang X, Hu Y (2018) Numerically investigating the optical properties of plasmonic metallic nanoparticles for effective solar absorption and heating. Sol Energy 161:17–24. https://doi.org/10.1016/j.solener.2017.12.032

[19] Pustovalov VK, Astafyeva LG, Fritzsche W (2015) Analysis of optical properties of spherical metallic nanoparticles for effective absorption of solar radiation and their heating. Sol Energy 122:1334–1341. https://doi.org/10.1016/j.solener.2015.09.022

[20] Singh D, Timofeeva EV, Moravek MR et al (2014) Use of metallic nanoparticles to improve the thermophysical properties of organic heat transfer fluids used in concentrated solar power. Sol Energy 105:468–478. https://doi.org/10.1016/j.solener.2014.02.036

[21] Wu S, Li Y, Ding W et al (2020) Recent advances of persistent luminescence nanoparticles in bioapplications. Nano-Micro Lett 12:1–26. https://doi.org/10.1007/s40820-020-0404-8

[22] Brus LE (1984) Electron-electron and electron-hole interactions in small semiconductor crystallites: the size dependence of the lowest excited electronic state. J Chem Phys 80:4403–4409. https://doi.org/10.1063/1.447218

[23] Ekimov AI, Efros AL, Onushchenko AA (1985) Quantum size effect in semiconductor microcrystals. Solid State Commun 88:947–950. https://doi.org/10.1016/0038-1098(93)90275-R

[24] Liz-Marzán LM (2006) Tailoring surface plasmons through the morphology and assembly of metal nanoparticles. Langmuir 22:32–41. https://doi.org/10.1021/la0513353

[25] Yen YC, Chen JA, Ou S et al (2017) Plasmon-enhanced photocurrent using gold nanoparticles on a three-dimensional TiO2 nanowire-web electrode. Sci Rep 7:1–8. https://doi.org/10.1038/srep42524

[26] Jain PK, Huang X, El-Sayed IH, El-Sayed MA (2008) Noble metals on the nanoscale: optical and photothermal properties and some applications in imaging, sensing, biology, and medicine. Acc Chem Res 41:1578–1586. https://doi.org/10.1021/ar7002804

[27] Lim WQ, Gao Z (2016) Plasmonic nanoparticles in biomedicine. Nano Today 11:168–188. https://doi.org/10.1016/j.nantod.2016.02.002

[28] Nanda KK, Maisels A, Kruis FE et al (2003) Higher surface energy of free nanoparticles. Phys Rev Lett 91:1–4. https://doi.org/10.1103/PhysRevLett.91.106102

[29] Xie D, Wang M, Cao L (2005) A simplified model to calculate the higher surface energy of free-standing nanocrystals. Phys Status Solidi Basic Res 242:76–78. https://doi.org/10.1002/pssb.200510036

[30] Taghizadeh S, Alimardani V, Roudbali PL et al (2019) Gold nanoparticles application in liver cancer. Photodiagnosis Photodyn Ther 25:389–400. https://doi.org/10.1016/j.pdpdt.2019.01.027

[31] Alzahrani HAH, Buckingham MA, Marken F, Aldous L (2019) Success and failure in the incorporation of gold nanoparticles inside ferri/ferrocyanide thermogalvanic cells. Electrochem commun 102:41–45. https://doi.org/10.1016/j.elecom.2019.03.007

[32] Liu X, Wang J, Ashby CR et al (2021) Gold nanoparticles: synthesis, physiochemical properties and therapeutic applications in cancer. Drug Discov Today. https://doi.org/10.1016/j.drudis.2021.01.030

[33] Tabatabaei MS, Islam R, Ahmed M (2021) Applications of gold nanoparticles in ELISA, PCR, and immuno-PCR assays: a review. Anal Chim Acta 1143:250–266. https://doi.org/10.1016/j.aca.2020.08.030

[34] Deshmukh SP, Patil SM, Mullani SB, Delekar SD (2019) Silver nanoparticles as an effective disinfectant: a review. Mater Sci Eng C 97:954–965. https://doi.org/10.1016/j.msec.2018.12.102

[35] Maharubin S, Zhou Y, Tan GZ (2019) Integration of silver nanoparticles and microcurrent for water filtration. Sep Purif Technol 212:57–64. https://doi.org/10.1016/j.seppur.2018.11.016

[36] Islam MA, Jacob MV, Antunes E (2021) A critical review on silver nanoparticles: from synthesis and applications to its mitigation through low-cost adsorption by biochar. J Environ Manage 281:111918. https://doi.org/10.1016/j.jenvman.2020.111918

[37] Choudhury H, Pandey M, Lim YPYQ et al (2020) Silver nanoparticles: advanced and promising technology in diabetic wound therapy. Mater Sci Eng C 112:110925. https://doi.org/10.1016/j.msec.2020.110925

[38] Camacho-Jiménez L, Álvarez-Sánchez AR, Mejía-Ruíz CH (2020) Silver nanoparticles (AgNPs) as antimicrobials in marine shrimp farming: a review. Aquac Reports 18:100512. https://doi.org/10.1016/j.aqrep.2020.100512

[39] Chaudhari PR, Masurkar SA, Shidore VB, Kamble SP (2012) Effect of biosynthesized silver nanoparticles on

Staphylococcus aureus biofilm quenching and prevention of biofilm formation. Int J Pharma Bio Sci 3:P222–P229. https://doi.org/10.1007/bf03353689

[40] Puja P, Kumar P (2019) A perspective on biogenic synthesis of platinum nanoparticles and their biomedical applications. Spectrochim Acta Part A Mol Biomol Spectrosc 211:94–99. https://doi.org/10.1016/j.saa.2018.11.047

[41] Dobrucka R (2019) Biofabrication of platinum nanoparticles using Fumariae herba extract and their catalytic properties. Saudi J Biol Sci 26:31–37. https://doi.org/10.1016/j.sjbs.2016.11.012

[42] Pourreza N, Abdollahzadeh R (2019) Colorimetric sensing of palladium ions based on in situ generation of palladium nanoparticles as an activator for the thionine-hydrazine reaction. Talanta 196:211–216. https://doi.org/10.1016/j.talanta.2018.12.050

[43] Garg G, Foltran S, Favier I et al (2020) Palladium nanoparticles stabilized by novel choline-based ionic liquids in glycerol applied in hydrogenation reactions. Catal Today 346:69–75. https://doi.org/10.1016/j.cattod.2019.01.052

[44] Wolfson A, Levy-Ontman O (2020) Development and application of palladium nanoparticles on renewable polysaccharides as catalysts for the Suzuki cross-coupling of halobenzenes and phenylboronic acids. Mol Catal 493:111048. https://doi.org/10.1016/j.mcat.2020.111048

[45] Li Z, Meng X (2020) Recent development on palladium enhanced photocatalytic activity: a review. J Alloys Compd 830:154669. https://doi.org/10.1016/j.jallcom.2020.154669

[46] Trzeciak AM, Augustyniak AW (2019) The role of palladium nanoparticles in catalytic C-C cross-coupling reactions. Coord Chem Rev 384:1–20. https://doi.org/10.1016/j.ccr.2019.01.008

[47] Vaid P, Raizada P, Saini AK, Saini RV (2020) Biogenic silver, gold and copper nanoparticles - a sustainable green chemistry approach for cancer therapy. Sustain Chem Pharm 16:100247. https://doi.org/10.1016/j.scp.2020.100247

[48] Ameh T, Sayes CM (2019) The potential exposure and hazards of copper nanoparticles: a review. Environ Toxicol Pharmacol 71:103220. https://doi.org/10.1016/j.etap.2019.103220

[49] Ojha NK, Zyryanov GV, Majee A et al (2017) Copper nanoparticles as inexpensive and efficient catalyst: a valuable contribution in organic synthesis. Coord Chem Rev 353:1–57. https://doi.org/10.1016/j.ccr.2017.10.004

[50] Ghuglot R, Titus W, Agnihotri AS et al (2021) Stable copper nanoparticles as potential antibacterial agent against aquaculture pathogens and human fibroblast cell viability.

Biocatal Agric Biotechnol 32:101932. https://doi.org/10.1016/j.bcab.2021.101932

[51] Pareek V, Bhargava A, Gupta R et al (2017) Synthesis and applications of noble metal nanoparticles: a review. Adv Sci Eng Med 9:527–544. https://doi.org/10.1166/asem.2017.2027

[52] Myroshnychenko V, Rodríguez-Fernández J, Pastoriza-Santos I et al (2008) Modelling the optical response of gold nanoparticles. Chem Soc Rev 37:1792–1805. https://doi.org/10.1039/b711486a

[53] Araujo TP, Quiroz J, Barbosa ECM, Camargo PHC (2019) Understanding plasmonic catalysis with controlled nanomaterials based on catalytic and plasmonic metals. Curr Opin Colloid Interface Sci 39:110–122. https://doi.org/10.1016/j.cocis.2019.01.014

[54] Wu B, Kuang Y, Zhang X, Chen J (2011) Noble metal nanoparticles/carbon nanotubes nanohybrids: synthesis and applications. Nano Today 6:75–90. https://doi.org/10.1016/j.nantod.2010.12.008

[55] Satishkumar BC, Vogl EM, Govindaraj A, Rao CNR (1996) The decoration of carbon nanotubes by metal nanoparticles. J Phys D Appl Phys 29:3173–3176. https://doi.org/10.1088/0022-3727/29/12/037

[56] Cai X-L, Liu C-H, Liu J et al (2017) Synergistic effects in CNTs-PdAu/Pt trimetallic nanoparticles with high electrocatalytic activity and stability. Nano-Micro Lett 9:48. https://doi.org/10.1007/s40820-017-0149-1

[57] Zhou Y-Y, Liu C-H, Liu J et al (2016) Self-decoration of ptni alloy nanoparticles on multiwalled carbon nanotubes for highly efficient methanol electro-oxidation. Nano-Micro Lett 8:371–380. https://doi.org/10.1007/s40820-016-0096-2

[58] Liu S, Zhou X-L, Zhang M-M et al (2016) Gold nanoparticles/carbon nanotubes composite microspheres for catalytic reduction of 4-nitrophenol. Chinese Chem Lett 27:843–846. https://doi.org/10.1016/j.cclet.2016.01.019

[59] Félix-Navarro RM, Beltrán-Gastélum M, Reynoso-Soto EA et al (2016) Bimetallic Pt–Au nanoparticles supported on multi-wall carbon nanotubes as electrocatalysts for oxygen reduction. Renew Energy 87:31–41. https://doi.org/10.1016/j.renene.2015.09.060

[60] Wei Y, Zhang X, Luo Z et al (2017) Nitrogen-doped carbon nanotube-supported pd catalyst for improved electrocatalytic performance toward ethanol electrooxidation. Nano-Micro Lett 9:1–9. https://doi.org/10.1007/s40820-017-0129-5

[61] Esquivel-Peña V, Bastos-Arrieta J, Muñoz M et al (2019) Metal nanoparticle–carbon nanotubes hybrid catalysts immobilized in a polymeric membrane for the reduction of

4-nitrophenol. SN Appl Sci 1:347. https://doi.org/10.1007/s42452-019-0357-z

[62] Guo Q, Fallon P, Yin J et al (2003) Growth of densely packed gold nanoparticles on graphite using molecular templates. Adv Mater 15:1084–1087. https://doi.org/10.1002/adma.200304938

[63] Tessonnier JP, Pesant L, Ehret G et al (2005) Pd nanoparticles introduced inside multi-walled carbon nanotubes for selective hydrogenation of cinnamaldehyde into hydrocinnamaldehyde. Appl Catal A Gen 288:203–210. https://doi.org/10.1016/j.apcata.2005.04.034

[64] Wang J, Lu SM, Li J, Li C (2015) A remarkable difference in CO2 hydrogenation to methanol on Pd nanoparticles supported inside and outside of carbon nanotubes. Chem Commun 51:17615–17618. https://doi.org/10.1039/c5cc07079a

[65] Lee M, Kim D (2016) Au nanoparticles attached carbon nanotubes as a high performance active element in field effect transistor. Mater Chem Phys 179:103–109. https://doi.org/10.1016/j.matchemphys.2016.05.015

[66] Ben Messaoud N, Ghica ME, Dridi C et al (2017) Electrochemical sensor based on multiwalled carbon nanotube and gold nanoparticle modified electrode for the sensitive detection of bisphenol A. Sensors Actuators B Chem 253:513–522. https://doi.org/10.1016/j.snb.2017.06.160

[67] Sun X, Qiao L, Wang X (2013) A novel immunosensor based on Au nanoparticles and polyaniline/multiwall carbon nanotubes/chitosan nanocomposite film functionalized interface. Nano-Micro Lett 5:191–201. https://doi.org/10.1007/BF03353750

[68] Magar HS, Ghica ME, Abbas MN, Brett CMA (2017) A novel sensitive amperometric choline biosensor based on multiwalled carbon nanotubes and gold nanoparticles. Talanta 167:462–469. https://doi.org/10.1016/j.talanta.2017.02.048

[69] Huff C, Dushatinski T, Abdel-Fattah TM (2017) Gold nanoparticle/multi-walled carbon nanotube composite as novel catalyst for hydrogen evolution reactions. Int J Hydrogen Energy 42:18985–18990. https://doi.org/10.1016/j.ijhydene.2017.05.226

[70] Che G, Lakshmi BB, Martin CR, Fisher ER (1999) Metal-nanocluster-filled carbon nanotubes: catalytic properties and possible applications in electrochemical energy storage and production. Langmuir 15:750–758. https://doi.org/10.1021/la980663i

[71] Yallappa S, Manjanna J, Dhananjaya BL et al (2016) Phytochemically functionalized cu and ag nanoparticles embedded in MWCNTs for enhanced antimicrobial and anticancer properties. Nano-Micro Lett 8:120–130. https://doi.org/10.1007/s40820-015-0066-0

[72] Wu H-QQ, Yuan P-SS, Xu H-YY et al (2006) Controllable synthesis and magnetic properties of Fe-Co alloy nanoparticles attached on carbon nanotubes. J Mater Sci 41:6889–6894. https://doi.org/10.1007/s10853-006-0935-5

[73] Melvin GJH, Ni Q-QQ, Suzuki Y, Natsuki T (2014) Microwave-absorbing properties of silver nanoparticle/carbon nanotube hybrid nanocomposites. J Mater Sci 49:5199–5207. https://doi.org/10.1007/s10853-014-8229-9

[74] Jiang MR, Zhou H, Cheng XH (2019) Effect of rare earth surface modification of carbon nanotubes on enhancement of interfacial bonding of carbon nanotubes reinforced epoxy matrix composites. J Mater Sci 54:10235–10248. https://doi.org/10.1007/s10853-019-03631-4

[75] Chen L, Xie H, Yu W (2012) Multi-walled carbon nanotube/silver nanoparticles used for thermal transportation. J Mater Sci 47:5590–5595. https://doi.org/10.1007/s10853-012-6451-x

[76] Ma H, Wang L, Chen L et al (2007) Pt nanoparticles deposited over carbon nanotubes for selective hydrogenation of cinnamaldehyde. Catal Commun 8:452–456. https://doi.org/10.1016/j.catcom.2006.07.020

[77] Ersen O, Werckmann J, Houllé M et al (2007) 3D electron microscopy study of metal particles inside multiwalled carbon nanotubes. Nano Lett 7:1898–1907. https://doi.org/10.1021/nl070529v

[78] Liu H, Zhang L, Wang N, Su DS (2014) Palladium nanoparticles embedded in the inner surfaces of carbon nanotubes: synthesis, catalytic activity, and sinter resistance. Angew Chemie - Int Ed 53:12634–12638. https://doi.org/10.1002/anie.201406490

[79] Wildgoose GG, Banks CE, Compton RG (2006) Metal nanoparticles and related materials supported on carbon nanotubes: methods and applications. Small 2:182–193. https://doi.org/10.1002/smll.200500324

[80] Bagheri H, Hajian A, Rezaei M, Shirzadmehr A (2017) Composite of Cu metal nanoparticles-multiwall carbon nanotubes-reduced graphene oxide as a novel and high performance platform of the electrochemical sensor for simultaneous determination of nitrite and nitrate. J Hazard Mater 324:762–772. https://doi.org/10.1016/j.jhazmat.2016.11.055

[81] Scarselli M, Camilli L, Castrucci P et al (2012) In situ formation of noble metal nanoparticles on multiwalled carbon nanotubes and its implication in metal–nanotube interactions. Carbon N Y 50:875–884. https://doi.org/10.1016/j.carbon.2011.09.048

[82] Gingery D, Bühlmann P (2008) Formation of gold nanoparticles on multiwalled carbon nanotubes by thermal evaporation. Carbon N Y 46:1966–1972. https://doi.org/10.1016/j.carbon.2008.08.007

[83] Penza M, Rossi R, Alvisi M et al (2009) Functional characterization of carbon nanotube networked films functionalized with tuned loading of Au nanoclusters for gas sensing applications. Sensors Actuators, B Chem 140:176–184. https://doi.org/10.1016/j.snb.2009.04.008

[84] Soin N, Roy SS, Karlsson L, McLaughlin JA (2010) Sputter deposition of highly dispersed platinum nanoparticles on carbon nanotube arrays for fuel cell electrode material. Diam Relat Mater 19:595–598. https://doi.org/10.1016/j.diamond.2009.10.029

[85] Tello A, Cárdenas G, Häberle P, Segura RA (2008) The synthesis of hybrid nanostructures of gold nanoparticles and carbon nanotubes and their transformation to solid carbon nanorods. Carbon N Y 46:884–889. https://doi.org/10.1016/j.carbon.2008.02.024

[86] Zhang C, Cui M, Ren J et al (2020) Facile synthesis of novel spherical covalent organic frameworks integrated with Pt nanoparticles and multiwalled carbon nanotubes as electrochemical probe for tanshinol drug detection. Chem Eng J 401:126025. https://doi.org/10.1016/j.cej.2020.126025

[87] Ou YY, Huang MH (2006) High-density assembly of gold nanoparticles on multiwalled carbon nanotubes using 1-pyrenemethylamine as interlinker. J Phys Chem B 110:2031–2036. https://doi.org/10.1021/jp055920o

[88] Yang D-Q, Hennequin B, Sacher E (2006) XPS Demonstration of π−π interaction between Benzyl mercaptan and multiwalled carbon nanotubes and their use in the adhesion of pt nanoparticles. Chem Mater 18:5033–5038. https://doi.org/10.1021/cm061256s

[89] Mu Y, Liang H, Hu J et al (2005) Controllable Pt nanoparticle deposition on carbon nanotubes as an anode catalyst for direct methanol fuel cells. J Phys Chem B 109:22212–22216. https://doi.org/10.1021/jp0555448

[90] Chen RJ, Zhang Y, Wang D, Dai H (2001) Noncovalent sidewall functionalization of single-walled carbon nanotubes for protein immobilization. J Am Chem Soc 123:3838–3839. https://doi.org/10.1021/ja010172b

[91] Ellis AV, Vijayamohanan K, Goswami R et al (2003) Hydrophobic anchoring of monolayer-protected gold nanoclusters to carbon nanotubes. Nano Lett 3:279–282. https://doi.org/10.1021/nl025824o

[92] del Río RS (2012) Non-covalent assembly of hybrid nanostructures of gold and palladium nanoparticles with carbon nanotubes. Int J Mater Res 103:901–905. https://doi.org/10.3139/146.110693

[93] Han L, Wu W, Kirk FL et al (2004) A direct route toward assembly of nanoparticle−carbon nanotube composite materials. Langmuir 20:6019–6025. https://doi.org/10.1021/la0497907

[94] Larimi A, Rahimi M, Khorasheh F (2020) Carbonaceous supports decorated with Pt–TiO2 nanoparticles using electrostatic self-assembly method as a highly visible-light active photocatalyst for CO2 photoreduction. Renew Energy 145:1862–1869. https://doi.org/10.1016/j.renene.2019.07.105

[95] Zhang S, Shao Y, Yin G, Lin Y (2010) Carbon nanotubes decorated with Pt nanoparticles via electrostatic self-assembly: a highly active oxygen reduction electrocatalyst. J Mater Chem 20:2826–2830. https://doi.org/10.1039/b919494k

[96] Hu X, Wang T, Qu X, Dong S (2006) In situ synthesis and characterization of multiwalled carbon nanotube/Au nanoparticle composite materials. J Phys Chem B 110:853–857. https://doi.org/10.1021/jp055834o

[97] Azamian BR, Coleman KS, Davis JJ et al (2002) Directly observed covalent coupling of quantum dots to single-wall carbon nanotubes. Chem Commun 2:366–367. https://doi.org/10.1039/b110690b

[98] Jeong G-H (2009) Surface functionalization of single-walled carbon nanotubes using metal nanoparticles. Trans Nonferrous Met Soc China 19:1009–1012. https://doi.org/10.1016/S1003-6326(08)60397-0

[99] Park H-S, Gong M-S (2012) Facile preparation of nanosilver-decorated MWNTs using silver carbamate complex and their polymer composites. Bull Korean Chem Soc 33:483–488. https://doi.org/10.5012/bkcs.2012.33.2.483

[100] Kim JY, Park K, Bae SY et al (2011) Preparation, characterization and catalytic properties of Pd-decorated carbon nanotubes possessing different linkers. J Mater Chem 21:5999–6005. https://doi.org/10.1039/c0jm03467c

[101] Kim JY, Jo Y, Kook S-KK et al (2010) Synthesis of carbon nanotube supported Pd catalysts and evaluation of their catalytic properties for CC bond forming reactions. J Mol Catal A Chem 323:28–32. https://doi.org/10.1016/j.molcata.2010.02.032

[102] Kim YT, Mitani T (2006) Surface thiolation of carbon nanotubes as supports: a promising route for the high dispersion of Pt nanoparticles for electrocatalysts. J Catal 238:394–401. https://doi.org/10.1016/j.jcat.2005.12.020

[103] Zanella R, Basiuk EV, Santiago P et al (2005) Deposition of gold nanoparticles onto Thiol-functionalized multiwalled carbon nanotubes. J Phys Chem B 109:16290–16295. https://doi.org/10.1021/jp0521454

[104] Sainsbury T, Stolarczyk J, Fitzmaurice D (2005) An experimental and theoretical study of the self-assembly of gold nanoparticles at the surface of functionalized multiwalled carbon nanotubes. J Phys Chem B 109:16310–16325. https://doi.org/10.1021/jp051224c

[105] Georgakilas V, Gournis D, Tzitzios V et al (2007) Decorating carbon nanotubes with metal or semiconductor nanoparticles. J Mater Chem 17:2679. https://doi.org/10.1039/b700857k

[106] Tessonnier J-P, Ersen O, Weinberg G et al (2009) Selective deposition of metal nanoparticles inside or outside multiwalled carbon nanotubes. ACS Nano 3:2081–2089. https://doi.org/10.1021/nn900647q

[107] Jin-Phillipp NY, Koch CT, van Aken PA (2011) Toward quantitative core-loss EFTEM tomography. Ultramicroscopy 111:1255–1261. https://doi.org/10.1016/j.ultramic.2011.02.006

[108] Xue B, Chen P, Hong Q et al (2001) Growth of Pd, Pt, Ag and Au nanoparticles on carbon nanotubes. J Mater Chem 11:2379–2382. https://doi.org/10.1039/b100618p

[109] Kiang C-HH, Goddard WA, Beyers R, Bethune DS (1995) Carbon nanotubes with single-layer walls. Carbon N Y 33:903–914. https://doi.org/10.1016/0008-6223(95)00019-A

[110] Ramírez-Meneses E, Montiel-Palma V, Chávez-Herrera VH, Reyes-Gasga J (2011) Decoration of single-walled carbon nanotubes with Pt nanoparticles from an organometallic precursor. J Mater Sci 46:3597–3603. https://doi.org/10.1007/s10853-011-5275-4

[111] Asadzadeh-Firouzabadi A, Zare HR (2018) Preparation and application of AgNPs/SWCNTs nanohybrid as an electroactive label for sensitive detection of miRNA related to lung cancer. Sens. Actu. B Chem 260:824–831. https://doi.org/10.1016/j.snb.2017.12.195

[112] Figueira CE, Moreira PF, Giudici R et al (2018) Nanoparticles of Ce, Sr, Co in and out the multi-walled carbon nanotubes applied for dry reforming of methane. Appl Catal A Gen 550:297–307. https://doi.org/10.1016/j.apcata.2017.11.019

[113] Guan Z, Lu S, Li C (2014) Enantioselective hydrogenation of α, β-unsaturated carboxylic acid over cinchonidine-modified Pd nanoparticles confined in carbon nanotubes. J Catal 311:1–5. https://doi.org/10.1016/j.jcat.2013.10.010

[114] Ajayan PM, Lijima S (1993) Capillarity-induced filling of carbon nanotubes. Nature 361:333–334. https://doi.org/10.1038/361333a0

[115] Lone MY, Kumar A, Ansari N et al (2018) Enhancement of sensor response of as fabricated SWCNT sensor with gold decorated nanoparticles. Sensors Actuators, A Phys 274:85–93. https://doi.org/10.1016/j.sna.2018.02.038

[116] Scarselli M, Castrucci P, Camilli L et al (2011) Influence of Cu nanoparticle size on the photo-electrochemical response from Cu-multiwall carbon nanotube composites. Nanotechnology. https://doi.org/10.1088/0957-4484/22/3/035701

[117] Duc Chinh V, Speranza G, Migliaresi C et al (2019) Synthesis of gold nanoparticles decorated with multiwalled carbon nanotubes (Au-MWCNTs) via cysteaminium chloride functionalization. Sci Rep 9:5667. https://doi.org/10.1038/s41598-019-42055-7

[118] Gebremariam TT, Chen F, Kou B et al (2020) PdAgRu nanoparticles on polybenzimidazole wrapped CNTs for electrocatalytic formate oxidation. Electrochim Acta 354:136678. https://doi.org/10.1016/j.electacta.2020.136678

[119] Ajayan PM, Stephan O, Redlich P, Colliex C (1995) Carbon nanotubes as removable templates for metal oxide nanocomposites and nanostructures. Nature 375:564–567. https://doi.org/10.1038/375564a0

[120] Dujardin E, Ebbesen TW, Hiura H, Tanigaki K (1994) Capillarity and wetting of carbon nanotubes. Science (80-) 265:1850–1852. https://doi.org/10.1126/science.265.5180.1850

[121] Segura RA, Contreras C, Henriquez R et al (2014) Gold nanoparticles grown inside carbon nanotubes: synthesis and electrical transport measurements. Nanoscale Res Lett 9:207. https://doi.org/10.1186/1556-276X-9-207

[122] Hevia S, Homm P, Cortes A et al (2012) Selective growth of palladium and titanium dioxide nanostructures inside carbon nanotube membranes. Nanoscale Res Lett 7:342. https://doi.org/10.1186/1556-276X-7-342

[123] Hajipour AR, Khorsandi Z, Farrokhpour H (2019) In situ synthesis of carbon nanotube-encapsulated cobalt nanoparticles by a novel and simple chemical treatment process: efficient and green catalysts for the Heck reaction. New J Chem 43:8215–8219. https://doi.org/10.1039/c9nj00813f

[124] Zhao Y, Tang Y, Star A (2013) Synthesis and functionalization of nitrogen-doped carbon nanotube cups with gold nanoparticles as cork stoppers. J Vis Exp. https://doi.org/10.3791/50383

[125] Zhao Y, Burkert SC, Tang Y et al (2015) Nano-gold corking and enzymatic uncorking of carbon nanotube cups. J Am Chem Soc 137:675–684. https://doi.org/10.1021/ja511843w

[126] Zhao Y, Tang Y, Chen Y, Star A (2012) Corking carbon nanotube cups with gold nanoparticles. ACS Nano 6:6912–6921. https://doi.org/10.1021/nn3018443

[127] Segura RA, Ibáñez W, Soto R et al (2006) Growth morphology and spectroscopy of multiwall carbon nanotubes synthesized by Pyrolysis of iron Phthalocyanine. J Nanosci Nanotechnol 6:1945–1953. https://doi.org/10.1166/jnn.2006.342

[128] Zhang XX, Wen GH, Huang S et al (2001) Magnetic properties of Fe nanoparticles trapped at the tips of the

aligned carbon nanotubes. J Magn Magn Mater 231:9–12. https://doi.org/10.1016/s0304-8853(01)00134-2

[129] Abrams ZR, Szwarcman D, Lereah Y et al (2007) Iron assisted growth of copper-tipped multi-walled carbon nanotubes. Nanotechnology. https://doi.org/10.1088/0957-4484/18/49/495602

[130] Ma Q, Wang D, Wu M et al (2013) Effect of catalytic site position: Nickel nanocatalyst selectively loaded inside or outside carbon nanotubes for methane dry reforming. Fuel 108:430–438. https://doi.org/10.1016/j.fuel.2012.12.028

[131] Shan B, Cho K (2006) First-principles study of work functions of double-wall carbon nanotubes. Phys Rev B - Condens Matter Mater Phys 73:081401. https://doi.org/10.1103/PhysRevB.73.081401

[132] Shaikh M, Balaraman E (2020) Confinement of nanoparticles in carbon nanotubes: A new paradigm in heterogeneous catalysis. In: Advanced Heterogeneous Catalysts Volume 1: Applications at the Nano-Scale. American Chemical Society, pp 459–481

[133] Chamberlain TW, Earley JH, Anderson DP et al (2014) Catalytic nanoreactors in continuous flow: hydrogenation inside single-walled carbon nanotubes using supercritical CO2. Chem Commun 50:5200–5202. https://doi.org/10.1039/c3cc49247h

[134] Wang YY, Rong Z, Wang YY et al (2015) Ruthenium nanoparticles loaded on multiwalled carbon nanotubes for liquid-phase hydrogenation of fine chemicals: an exploration of confinement effect. J Catal 329:95–106. https://doi.org/10.1016/j.jcat.2015.04.034

[135] Labulo AH, Martincigh BS, Omondi B, Nyamori VO (2017) Advances in carbon nanotubes as efficacious supports for palladium-catalysed carbon–carbon cross-coupling reactions. J Mater Sci 52:9225–9248. https://doi.org/10.1007/s10853-017-1128-0

[136] Ravindra R, Bhat BR (2012) Hydrogen storage in palladium decorated carbon nanotubes prepared by solventless method. Int. J. Appl. Phys. Mathemat. 2:63–66

[137] Mukkamala SB (2021) Hydrogen Storage Performance of Metal Nanoparticle Decorated Multi-walled Carbon Nanotubes. Carbon Related Materials. Springer, Singapore, pp 103–125

[138] Star A, Joshi V, Skarupo S et al (2006) Gas sensor array based on metal-decorated carbon nanotubes. J Phys Chem B 110:21014–21020. https://doi.org/10.1021/jp064371z

[139] Krishna Kumar M, Ramaprabhu S (2006) Nanostructured Pt functionlized multiwalled carbon nanotube based hydrogen sensor. J Phys Chem B 110:11291–11298. https://doi.org/10.1021/jp0611525

[140] Kazakova MA, Andreev AS, Selyutin AG et al (2018) Co metal nanoparticles deposition inside or outside multi-walled carbon nanotubes via facile support pretreatment. Appl Surf Sci 456:657–665. https://doi.org/10.1016/j.apsusc.2018.06.124

[141] Andreev AS, Kazakova MA, Ishchenko AV et al (2017) Magnetic and dielectric properties of carbon nanotubes with embedded cobalt nanoparticles. Carbon N Y 114:39–49. https://doi.org/10.1016/j.carbon.2016.11.070

[142] Pham-Huu C, Keller N, Ehret G et al (2001) Carbon nanofiber supported palladium catalyst for liquid-phase reactions. J Mol Catal A Chem 170:155–163. https://doi.org/10.1016/S1381-1169(01)00055-3

[143] Gallezot P, Richard D (1998) Selective hydrogenation of α,β-unsaturated aldehydes. Catal Rev 40:81–126. https://doi.org/10.1080/01614949808007106

[144] Coq B, Figueras F (1998) Structure - Activity relationships in catalysis by metals: some aspects of particle size, bimetallic and supports effects. Coord Chem Rev 178–180:1753–1783. https://doi.org/10.1016/s0010-8545(98)00058-7

[145] Toebes ML, Prinsloo FF, Bitter JH et al (2003) Influence of oxygen-containing surface groups on the activity and selectivity of carbon nanofiber-supported ruthenium catalysts in the hydrogenation of cinnamaldehyde. J Catal 214:78–87. https://doi.org/10.1016/S0021-9517(02)00081-7

[146] Delbecq F, Sautet P (1995) Competitive C=C and C=O adsorption of α-β-unsaturated Aldehydes on Pt and Pd Surfaces in relation with the selectivity of hydrogenation reactions: a theoretical approach. J Catal 152:217–236. https://doi.org/10.1006/jcat.1995.1077

[147] Ravasio N, Rossi M (1991) Selective hydrogenations promoted by copper catalysts. 1. chemoselectivity, regioselectivity, and stereoselectivity in the hydrogenation of 3-substituted steroids. J Org Chem 56:4329–4333. https://doi.org/10.1021/jo00013a054

[148] Pak AM, Konuspaev SR, Zakumbaeva GD, Sokolskii DV (1981) Hydrogenation of citral to citronellol over Ni−Cr2O3. React Kinet Catal Lett 16:339–343. https://doi.org/10.1007/BF02066587

[149] Pan J, Shen S, Zhou W et al (2020) Recent progress in photocatalytic hydrogen evolution. Wuli Huaxue Xuebao/Acta Phys - Chim Sin. https://doi.org/10.3866/PKU.WHXB201905068

[150] Olabi AGG, Bahri Saleh A, Abdelghafar AA et al (2020) Large-vscale hydrogen production and storage technologies: current status and future directions. Int J Hydrogen Energy. https://doi.org/10.1016/j.ijhydene.2020.10.110

[151] Dixit S (2020) Solar technologies and their implementations: a review. Mater Today Proc 28:2137–2148. https://doi.org/10.1016/j.matpr.2020.04.134

[152] Agathokleous RA, Kalogirou SA (2020) Status, barriers and perspectives of building integrated photovoltaic systems. Energy 191:116471. https://doi.org/10.1016/j.energy.2019.116471

[153] Chen X, Ali I, Song L et al (2020) A review on recent advancement of nano-structured-fiber-based metal-air batteries and future perspective. Renew Sustain Energy Rev 134:110085. https://doi.org/10.1016/j.rser.2020.110085

[154] Bin D, Yang B, Li C et al (2018) In situ growth of nife alloy nanoparticles embedded into N-Doped bamboo-like carbon nanotubes as a bifunctional electrocatalyst for Zn-air batteries. ACS Appl Mater Interf 10:26178–26187. https://doi.org/10.1021/acsami.8b04940

[155] Li P, Zhao R, Chen H et al (2019) Recent advances in the development of water oxidation electrocatalysts at mild pH. Small 15:1805103. https://doi.org/10.1002/smll.201805103

[156] Dou S, Tao L, Huo J et al (2016) Etched and doped Co 9 S 8 /graphene hybrid for oxygen electrocatalysis. Energy Environ Sci 9:1320–1326. https://doi.org/10.1039/C6EE00054A

[157] Forsythe RC, Müller AM (2020) Quo vadis water oxidation? Catal Today. https://doi.org/10.1016/j.cattod.2020.06.011

[158] Dong Y, Oloman CW, Gyenge EL et al (2020) Transition metal based heterogeneous electrocatalysts for the oxygen evolution reaction at near-neutral pH. Nanoscale 12:9924–9934. https://doi.org/10.1039/D0NR02187C

[159] Lyu F, Wang Q, Choi SM, Yin Y (2019) Noble-metal-free electrocatalysts for oxygen evolution. Small 15:1804201. https://doi.org/10.1002/smll.201804201

[160] Han L, Dong S, Wang E (2016) Transition-metal (Co, Ni, and Fe)-based electrocatalysts for the water oxidation reaction. Adv Mater 28:9266–9291. https://doi.org/10.1002/adma.201602270

[161] Li A, Sun Y, Yao T, Han H (2018) Earth abundant transition metal based electrocatalysts for water electrolysis to produce renewable hydrogen. Chem A Eur J. 24:18334–18355. https://doi.org/10.1002/chem.201803749

[162] Zhou H, Li X, Li Y et al (2019) Applications of MxSey (M = Fe Co, Ni) and their composites in electrochemical energy storage and conversion. Nano-Micro Lett 11:40. https://doi.org/10.1007/s40820-019-0272-2

[163] Liu Y, Jiang H, Zhu Y et al (2016) Transition metals (Fe Co, and Ni) encapsulated in nitrogen-doped carbon nanotubes as bi-functional catalysts for oxygen electrode reactions. J Mater Chem A 4:1694–1701. https://doi.org/10.1039/c5ta10551j

[164] Jin C, Lu F, Cao X et al (2013) Facile synthesis and excellent electrochemical properties of NiCo 2O4 spinel nanowire arrays as a bifunctional catalyst for the oxygen reduction and evolution reaction. J Mater Chem A 1:12170–12177. https://doi.org/10.1039/c3ta12118f

[165] Chen Z, Chen Z, Yu A et al (2012) Manganese dioxide nanotube and nitrogen-doped carbon nanotube based composite bifunctional catalyst for rechargeable zinc-air battery. Electrochim Acta 69:295–300. https://doi.org/10.1016/j.electacta.2012.03.001

[166] Yu J, Zhong Y, Zhou W, Shao Z (2017) Facile synthesis of nitrogen-doped carbon nanotubes encapsulating nickel cobalt alloys 3D networks for oxygen evolution reaction in an alkaline solution. J Power Sources 338:26–33. https://doi.org/10.1016/j.jpowsour.2016.11.023

[167] Hou Y, Cui S, Wen Z et al (2015) Strongly coupled 3D hybrids of N-doped porous carbon nanosheet/CoNi alloy-encapsulated carbon nanotubes for enhanced electrocatalysis. Small 11:5940–5948. https://doi.org/10.1002/smll.201502297

[168] Wen F, Zhang F, Liu Z (2011) Investigation on microwave absorption properties for multiwalled carbon Nanotubes/Fe/Co/Ni nanopowders as lightweight absorbers. J Phys Chem C 115:14025–14030. https://doi.org/10.1021/jp202078p